



1 **Use of automatic radiosonde launchers to measure temperature and humidity**
2 **profiles from the GRUAN perspective**

3
4 Fabio Madonna¹, Rigel Kivi², Jean-Charles Dupont³, Bruce Ingleby⁴, Masatomo Fujiwara⁵, Gonzague
5 Romanens⁶, Miguel Hernandez⁷, Xavier Calbet⁷, Marco Rosoldi¹, Aldo Giunta¹, Tomi Karppinen²,
6 Masami Iwabuchi⁸, Shunsuke Hoshino⁹, Christoph von Rohden¹⁰, Peter William Thorne¹¹

- 7
8 ¹Consiglio Nazionale delle Ricerche - Istituto di Metodologie per l'Analisi Ambientale (CNR-IMAA), Tito Scalo (Potenza), Italy
9 ²Finnish Meteorological Institute, Helsinki, Finland
10 ³Institut Pierre et Simon Laplace (IPSL), Paris, France
11 ⁴European Centre for Medium-range Weather Forecasts (ECWMF), Reading, UK
12 ⁵Hokkaido University, Sapporo, Japan
13 ⁶MeteoSwiss, Payerne, Switzerland
14 ⁷Agencia Estatal de Meteorología, Madrid, Spain
15 ⁸Japan Meteorological Agency (JMA), Tokyo, Japan.
16 ⁹Aerological Observatory, Tsukuba, Ibaraki, Japan.
17 ¹⁰Deutscher Wetterdienst (DWD), GRUAN Lead Centre, Lindenberg, Germany.
18 ¹¹Irish Climate Analysis and Research Units, Dept. of Geography, Maynooth University, Maynooth, Ireland.

19
20 **Abstract**

21 In the last two decades, technological progress has not only seen improvements to the quality of
22 atmospheric upper-air observations, but also provided the opportunity to design and implement
23 automated systems able to replace measurement procedures typically performed manually.
24 Radiosoundings, which remain one of the primary data sources for weather and climate
25 applications, are still largely performed around the world manually, although increasingly fully
26 automated upper-air observations are used, from urban areas to the remotest locations, which
27 minimise operating costs and challenges in performing radiosounding launches. This analysis
28 presents a first step to demonstrating the reliability of the Automatic Radiosonde Launchers (ARLs)
29 provided by Vaisala, Meteomodem and Meisei. The metadata and datasets collected by a few
30 existing ARLs operated by GRUAN certified or candidate sites (Sondakyla, Payerne, Trappes,
31 Potenza) have been investigated and a comparative analysis of the technical performance (i.e.
32 manual vs ARL) is reported. The performance of ARLs is evaluated as being similar or superior to
33 those achieved with the traditional manual launches in terms of percentage of successful launches,
34 balloon burst and ascent speed. For both temperature and relative humidity, the ground check
35 comparisons showed a negative bias of a few tenths of a degree and % RH, respectively. Two
36 datasets of parallel soundings between manual and ARL-based measurements, using identical sonde
37 models, provided by Sodankylä and Faa'a stations showed mean differences between the ARL and
38 manual launches smaller than ± 0.2 K up to 10 hPa for the temperature profiles. For relative
39 humidity, differences were smaller than 1% RH for the Sodankylä dataset up to 300 hPa, while they
40 were smaller than 0.7% RH for Faa'a station. Finally, the O-B mean and rms statistics for German



41 RS92 and RS41 stations which operate a mix of manual and ARL launch protocols, calculated using
42 the ECMWF forecast model, are very similar, although RS41 shows larger rms(O-B) differences for
43 ARL stations, in particular for temperature and wind. A discussion on the potential next steps
44 proposed by GRUAN community and other parties is provided, with the aim to lay the basis for the
45 elaboration of a strategy to fully demonstrate the value of ARLs and guarantee that the provided
46 products are traceable and suitable for the creation of GRUAN data products.

47

48 **1. Introduction**

49 Radiosondes are one of the primary sources of upper-air data for weather and climate monitoring.
50 Despite the advent and the fast integration of GPS-RO (radio occultation) as an effective source of
51 upper-air temperature data (Ho et al., 2017), radiosondes will likely remain an indispensable source
52 of free-atmosphere observational data into the future. Radiosonde observations are applied to a
53 broad spectrum of applications, being input data for weather prediction models and global
54 reanalysis, nowcasting, pollution and radiative transfer models, monitoring data for weather and
55 climate change research, and ground reference for satellite and also for other in-situ and remote
56 sensing profiling data.

57 The analysis of historical radiosonde data archives has repeatedly highlighted that changes in
58 operational radiosondes introduce clear discontinuities in the collected time series (Thorne et al.,
59 2005; Sherwood et al., 2008; Haimberger et al., 2011). Moreover, where radiosonde observations
60 have been used in numerical weather prediction, systematic errors have sometimes been
61 disregarded and the instrumental uncertainties have been estimated in a non-rigorous way
62 (Carminati et al., 2019). Nowadays, there is a broad consensus on the need to have reference
63 measurements with quantified traceable uncertainties for scientific and user-oriented applications.
64 The GCOS Reference upper-air network (GRUAN) provides fundamental guidelines for establishing
65 and maintaining reference-quality atmospheric observations which are based on principal concepts
66 of metrology, in particular, traceability (Bodeker et al., 2016).

67 Apart from direct instrument performance aspects of the radiosounding equipment and radiosonde
68 model, it must be acknowledged that there are many challenges in performing radiosounding
69 launches. During the preparation and launch phase, many circumstances may interfere with the
70 smooth operation of radiosoundings such as undertaking launches at night, harsh meteorological
71 conditions for balloon train preparation compounded by basic equipment in the balloon shelter, if
72 any, and safe handling when using hydrogen as balloon gas, and last but not least the risk of
73 errors/mishandling by the operators. Additional expenditure may be required when observations



74 are performed in remote regions of the globe, including the polar regions, deserts, or remote
75 islands.

76 Since the start of radiosounding efforts in the early-to-mid 20th Century, the radiosounding systems
77 and the radiosondes themselves have radically changed in size, weight, performance. For example,
78 a very important progress was the automation of the data processing and message production from
79 about 1980. Of particular note is that thanks to new technologies, over recent decades, three
80 manufacturers have developed and deployed fully Automatic Radiosonde Launchers (ARL) able to
81 perform unmanned soundings.

82 ARL are robotic systems able to complete in an automatic fashion almost all of the operations
83 performed manually by an operator during radiosounding launch preparation and release, including
84 the implementation of ground check procedures. The advantages of ARLs are in the reduction of
85 the challenges described above as well as in the reduced running costs of a sounding station (e.g.
86 reduction in the need for trained staff and the trend of automating hydrogen production due to cost
87 reasons and to the helium international crisis) and in ameliorating problems of recruiting long-term
88 operators for remote locations. Nevertheless, it must be also stressed that the system must be
89 regularly stocked and maintained to avoid major issues and high repair costs being incurred. In
90 addition, with changes in the radiosonde technology, updates of the systems might be required to
91 enable the use of a new radiosonde type, with periodical costs (variable, every 3-6 years) which
92 might be substantial for a station. In 2018, NOAA-NCEI published stories on its website which show
93 the potential benefits of using ARLs (<http://www.noaa.gov/stories/up-up-and-away-6-benefits-of-automated-weather-balloon-launches>). Within these stories as well as from the feedback collected
94 within the GRUAN community, several radiosonde stations have reported benefits from the use of
95 ARL and an increase in the percentage of successful soundings with a potential reduction of missing
96 data in the collected data records.

98 Using recent ECMWF statistics on the number of stations transmitting data to the WMO Information
99 System (WIS) and information provided by the GRUAN community and others, there are about 90
100 ARLs (Figure 1) providing data versus about 700 manual stations. ARL stations cover many countries
101 and remote regions, including Arctic and Antarctic locations as well as a broad suite of remote Pacific
102 and other island locations. As far as is known many of the ARL stations only make automated
103 launches. In addition, there are a few more stations, used by research institutions or environmental
104 agencies, not transmitting data via the Global Telecommunication System (GTS) of the WMO



105 Information System (WIS). The total number of stations operating an ARL worldwide has increased
106 within the last decade (see Table A1 and A2 in Appendix A).

107 Vaisala introduced its first automatic system in 1990, Meisei in 2006 and Meteomodem in 2009.
108 Despite their relatively recent development and deployment, ARLs appear to be successful, and the
109 number of deployed systems will likely increase in the future. However, to date there are very few
110 peer-reviewed papers in the literature dealing with ARLs or comparing ARL vs manual data (often
111 limited to specific examples, e.g. Madonna et al., 2011). More specifically, there is currently no side-
112 by-side assessment of quality in comparison to manually launched sondes. The aim of this paper is
113 thus to quantify the reliability and stability of ARLs and assess the accuracy of their data compared
114 to the traditional manual systems. A discussion on the measurement traceability and on the
115 feasibility to use ARLs in a regular way in the GCOS Reference Upper Air Network (www.gruan.org)
116 is also provided. At present, traceability to SI standards is quantified at several GRUAN sites by the
117 use of a Standard Humidity Chamber (SHC) which can be used for ARL before the launch loading
118 only. The SHC is a simple ventilated chamber ($\sim 4 - 5$ m/s) using distilled water which, during the
119 ground check procedure, is first heated a few degrees above ambient temperature and then cooled
120 to saturate air at 100% relative humidity. The SHC allows a check of each radiosonde at 100% RH
121 using distilled water (or other RH values using solutions with specific salts although these are
122 generally only used at the GRUAN Lead Centre and for sonde characterisation and not operational
123 sounding preparation purposes).

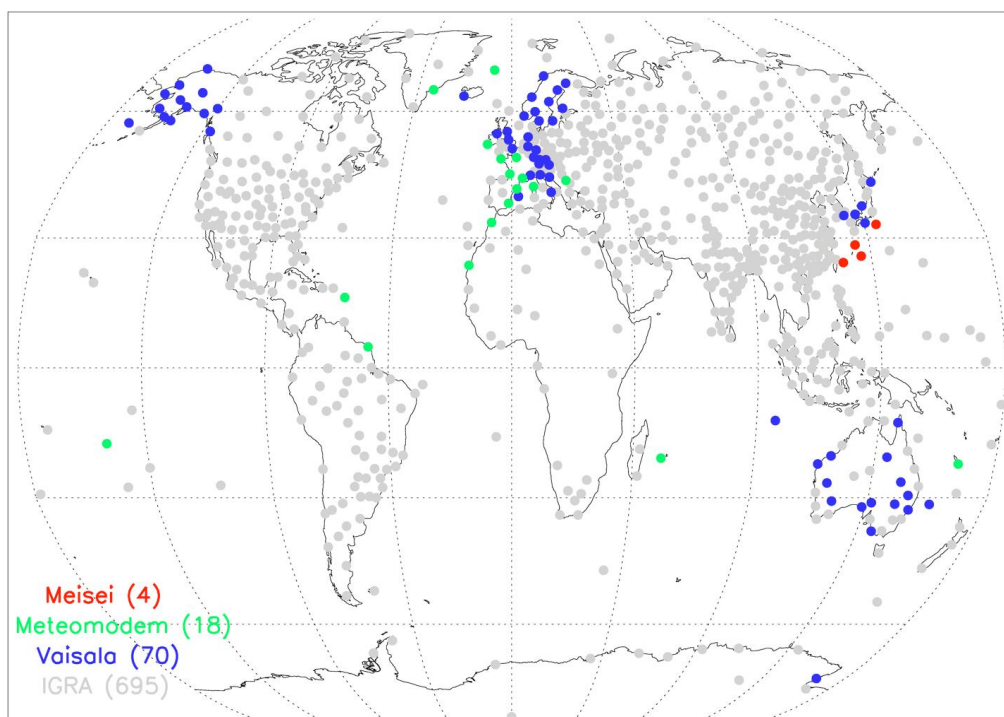
124 The comparison reported in this paper focuses exclusively on temperature and relative humidity
125 profiles and rely upon manufacturer's products (i.e. GRUAN Data Processing based on the raw data
126 collected by the sonde, described in Dirksen et al., 2014, and Kobayashi et al., 2019, is not used).

127 The remainder of the paper is structured as follows. In section 2, a short description of the three
128 ARLs is provided. In section 3, the technical performance of the ARLs is investigated on the basis of
129 statistics comparing the technical efficiency of the ARLs versus the manual sounding stations as well
130 as reporting an analysis of the feedback from station operators collected at the GRUAN sites on the
131 advantages, limitations and technical issues faced to maintain and ensure continuity of ARL
132 operations. Section 4 reports on the effect of the usage of ARLs on the stability and the accuracy of
133 ground-check calibration procedures. Section 5 provides statistics obtained from parallel soundings
134 at different sites for both temperature and humidity profiles. Section 6 discusses the comparison
135 between observation-minus-background (O-B) statistics obtained from ARL data and manually
136 launched data, respectively, using the ECMWF short-range forecast fields. Finally, section 7 provides



137 a summary and a description of the experiments which might be performed to design future ARL
138 setup to enable full measurement system traceability to SI units and, therefore, to meet GRUAN
139 requirements for long term reference climate data.

140



141

142 Figure 1: Map of stations running an Automatic Radiosonde Launcher (ARL) and transmitting the data to the WIS in late
143 2019 (see also Appendix A). Blue dots are the Vaisala ARL, green the Meteomodem, and red the Meisei. In light grey,
144 the manual station providing data to the WIS in September are also reported. Number of stations for each color is
145 reported in brackets.

146

147 2. Description of existing ARL systems

148

149 2.1 Vaisala Autosonde: brief history and recent system configurations

150 Automation of upper-air sounding data processing has made steady progress since the early 1970's
151 and is now widespread (Kostamo, P., 1992). The Vaisala Autosonde project was started in late 1992
152 and a working prototype presented at CIMO, Vienna, in 1993. The prototype was tested in Norway
153 and Sweden in 1993 and 1994. This coincided with the replacement of manual balloon tracking
154 systems by Omega and Loran networks. It was provided by Vaisala Oy (Finland) and was installed at
155 the Landvetter station in Sweden in 1994. As of today, about 80 Vaisala ARLs have been installed



156 worldwide and the number of soundings performed has exceeded 800,000, while the annual
157 number of new soundings will soon exceed 70,000 (Lilja et al., 2018). With the newest Autosonde
158 model it is possible to perform 60 soundings without replenishment, while the earlier models
159 allowed up to 24 soundings.

160 The first radiosonde type used for an automatic launch was the RS80-15N (during 1994-2006). The
161 RS80 radiosonde was followed by the models RS92 (manufactured 2005-2017) and then RS41
162 (available since late 2013). The RS92 radiosonde (Dirksen et al. 2014) which performs
163 measurements with a nominal measurement uncertainty (provided by the manufacturer) of 0.5°C
164 for temperature, 1.0 hPa for pressure below 100 hPa and 0.6 hPa above, 0.15 m s⁻¹ for wind speed
165 and 5 % RH or relative humidity ([https://www.vaisala.com/sites/default/files/documents/RS92SGP-](https://www.vaisala.com/sites/default/files/documents/RS92SGP-Datasheet-B210358EN-F-LOW.pdf)
166 [Datasheet-B210358EN-F-LOW.pdf](https://www.vaisala.com/sites/default/files/documents/RS92SGP-Datasheet-B210358EN-F-LOW.pdf)). RS41 sonde specifications for nominal measurement
167 uncertainties (provided by the manufacturer) are 0.3°C for temperatures below 16 km and 0.4°C
168 above, 0.01 hPa for pressure sensor, 0.15 m s⁻¹ for wind speed and 4 % RH for relative humidity
169 (<https://www.vaisala.com/sites/default/files/documents/RS41-SGP-Datasheet-B211444EN.pdf>).

170 Note that the Vaisala RS41 radiosondes are of two different types: RS41-SG which are not equipped
171 with a pressure sensor and using the GPS-based method to infer pressure (Lehtinen, 2014), and
172 RS41-SGP which uses a pressure sensor as the default. More stations use the RS41-SGP than the
173 RS41-SG: in November 2019, 158 stations type RS41-SGP versus 66 stations using type RS41-SGP.

174 To launch the RS41 sondes, the Autosonde Ground Check (GC) procedure has been updated. The
175 GC device of the RS41 sondes consists of a wall-mounted box and an activator that contains a
176 wireless reader for the radiosonde. The device is designed to automatically activate the radiosonde
177 and to enable wireless data transfer. An activator is connected to the reader box with a coaxial
178 cable. The ground check device also includes a barometer while the surface pressure used as a
179 reference for the launch is obtained from a separate co-located automatic weather station.

180 However, the ground check pressure device can be used as a backup for the weather station sensor.
181 The GC performs a temperature check where the actual temperature sensor is compared with the
182 one integrated on the humidity sensor chip. In contrast to the RS92 GC, a pre-flight fine-tuning of
183 the temperature measurement is no longer applied to the RS41 because the manufacturer found
184 that the accuracy of the RS41 temperature measurement is practically unchanged during storage.

185 Humidity is also checked in the GC. The RS41 humidity check consists of two main steps – the sensor
186 reconditioning phase and the 0% RH check. In the reconditioning phase, the sensor is heated to
187 remove possible contaminants that might affect the measurement results and cause a slight

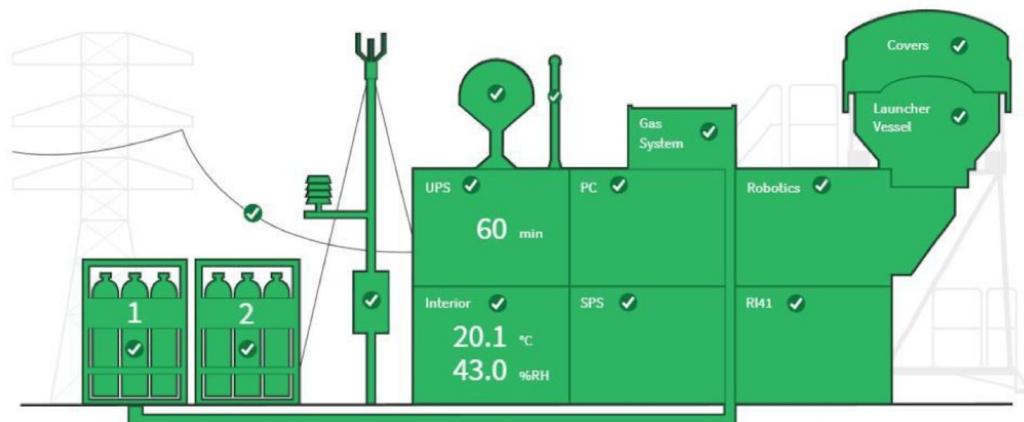


188 degradation of the sensitivity of the humidity sensor. Then, the humidity sensor is checked and then
189 corrected against a dry humidity condition. Specifically, the dry reference condition of the new zero
190 humidity check is generated in open air by heating the sensor using the integrated heating element
191 on the sensor chip. The procedure is based on the decrease of relative humidity towards zero as the
192 temperature rises high enough. This method differs from the RS92 GC where the correction was
193 based on a dry condition generated with desiccants, whose drying capacity gradually fades with the
194 time.

195 The radiosonde's humidity sensor is reconditioned and ground check performed during the
196 automated launch preparation in order to ensure same performance as in manual stations (Lilja et
197 al., 2018). The top panel of Figure 2 provides a schematic picture of the most recent VAISALA AS41
198 Autosonde system configuration while the bottom panel shows a photograph of the Autosonde
199 system operational at the Finnish Meteorological Institute GRUAN site in Sodankylä (WIGOS station
200 identifier=0-20000-0-02836, 67.34 °N, 26.63 °E, 179 m a.s.l.). In Table 1, the basic technical data of
201 the Autosonde AS41 are reported. More details on the specifications of the Vaisala Autosonde AS41
202 can be found in the datasheet (B211636EN-A_2 pages.pdf, last accessed September 20, 2019)
203 available on the Vaisala website (<https://www.vaisala.com>).

204

205



206
207
208
209
210
211
212
213
214
215
216

Figure 2: Schematics of the VAISALA Autosonde AS41 system in its most recent configuration (top panel), and photo of the Autosonde system AS15 (bottom panel) operational at the Finnish Meteorological Institute GRUAN site in Sodankylä (WIGOS station identifier=0-20000-0-02836, 67.34 °N, 26.63 °E, 179 m a.s.l., see Vaisala 2018, https://www.vaisala.com/sites/default/files/documents/AUTOSONDE%20AS41%20Datashet%20B211636EN-A_2%20pages.pdf).



217

Table 1: Autosonde AS41 technical data (Vaisala, 2018)

Dimensions	Width: 3.30 m
	Length: 7.80 m
Launch Tube Diameter	2.20 m
Height during transport	2.90 m
Total height with launcher tube	5.10 m
Gross weight with launcher tube	7.5 t
Electrical energy consumption	< 1 kW (without air conditioning)

218

219

220 2.2 Meteomodem Robotsonde

221 The Meteomodem ARL is an automatic balloon launcher system that can perform up to 12 or 24
222 soundings without any manual control (<http://www.Meteomodem.com/docs/en/Leaflet-robotsonde.pdf>). The system is compatible with M10 and M20 Meteomodem radiosonde types. It
223 is built in a robust dry maritime container and composed of the following subsystems (Figure 3):
224

- 225 • Operator room with electronic control unit and PC workstation, isolated from the launch tube
226 by an air-tight safety door, and used only during radiosonde setup and restocking;
- 227 • Carrousel with 12 or 24 removable containers for balloon trains, and with individual flexible
228 cover on balloon locations which preserve balloons from desiccation;
- 229 • Launch tube for balloon inflation and release and pneumatic equipment or pressurized air
230 network;
- 231 • Optionally, a double-door entrance to protect from strong winds, rain, drifting snow or
232 sandstorms.

233 The Meteomodem ARL main specifications are reported in Table 2. Worldwide there are 19
234 Meteomodem ARL systems automatically launching Meteomodem M10 radiosondes. The
235 specifications for nominal measurement uncertainties (provided by the manufacturer) are 0.58°C
236 for temperature, 1 hPa for pressure, 0.15 m s⁻¹ for wind speed and 5 % RH for relative humidity
237 (www.Meteomodem.com/docs/en/Leaflet-m10.pdf).

238



239

Table 2: Meteomodem ARL specifications

Dimensions	Width: 2.44 m
	Length: 6.00 m
Launch Tube Diameter	2.00 m
Height during transport	3.10 m
Total height with launcher tube	3.60 m
Gross weight with launcher tube	3.5 t
Electrical energy consumption	< 1 kW (without air conditioning)

240

241

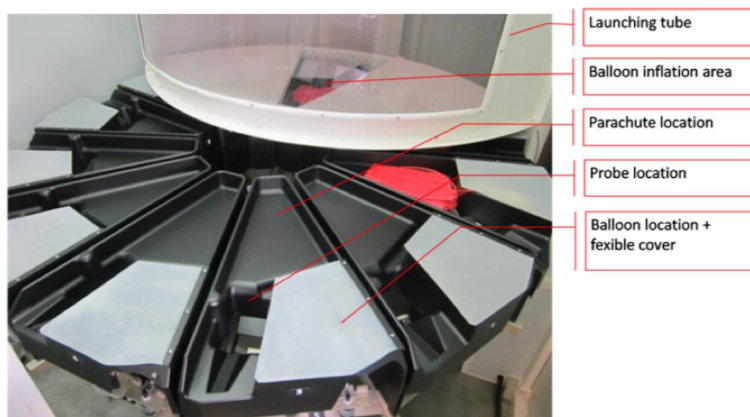
242 For each launch, there is a preparation phase which comprises the radiosonde GC and the loading
243 of the balloon train (with the radiosonde, the unwinder, the parachute, and the balloon) into
244 individual bins before finally sounding parameters (e.g. launch time schedule, inflation volume, etc.)
245 are setup.

246 During the launch phase, before powering on the sonde, the system performs a scan of the
247 bandwidth in order to detect possible radio interference, then the radiosonde battery pack is
248 powered on through an infrared link. According to the scan result, the system sets up the new
249 frequency through an infrared link, and GNSS signal collection is initialized. Then, the system loads
250 the calibration data of the relevant radiosonde stored during the preparation phase and checks
251 consistency with PTU criteria. The Meteomodem ARL GC is a standard Meteomodem GC which
252 consists in a sealed box enclosing a reference and a fan which homogenised the inside temperature
253 and relative humidity. It is recommended to return the Meteomodem GC every 3 years for
254 calibration. The calibration is made with a certified Rotronic HC2A-S probe.

255 Then, the ARL records the ground check data and the metadata. Balloon inflation starts accordingly:
256 the system monitors a flowmeter to inflate the balloon to the specified volume. The ARL may use
257 either helium or hydrogen gas. Finally, the balloon is released at the specified launch time. In case
258 of launch failure before balloon release or during the flight, the procedure will restart for a new
259 sounding immediately or can alternatively be manually launched according to a preset time
260 schedule. At any time, an immediate start of the launch procedure can be initiated by an operator
261 (locally or remotely).

262

263



264
265
266
267
268
269

Figure 3: Meteomodem Robotsonde (top panel) launching a balloon at Trappes station (WIGOS station identifier=0-20000-0-07145, 48.46N, 0.20E, 168 m asl, <http://www.Meteomodem.com/robotsonde.html>) and photograph of the carousel of Meteomodem Robotsonde with the balloon location (bottom panel).

270 For those stations operating an ARL and adopting a protocol based on GRUAN recommendations
271 (Dirksen et al., 2014), as at Trappes station (WIGOS station identifier=0-20000-0-07145, 48.46N,
272 0.20E, 168 m asl, top panel of Figure 2.2), the GRUAN M10 ground check procedure is performed in
273 two steps: 5 minutes in a ventilated hut in ambient conditions together with calibrated T and RH
274 sensors and, further, another 5 minutes to test the radiosonde performance in the SHC. Then each
275 radiosonde is loaded in the ARL carousel (bottom panel of Figure 3).



276 A technical document describing the M10 sensor, corrections and uncertainties for both the
277 temperature and relative humidity sensors will become available through the GRUAN community
278 as soon as a Meteomodem M10 GRUAN data product is available.

279

280 **2.3 Meisei Automated Radiosonde System**

281 The Meisei ARL, named “Automated Radiosonde System” is designed for fail-safe operation and
282 high remote operability. Compared to the previous version developed in 2006, the new system is
283 able to load more radiosondes thanks to the development of the Meisei “Canister Type”. The
284 operator can preload a maximum number of 40 sondes adjustable in the so-called "Canister
285 modules". The canister has been recently implemented to reduce failures. Once the launch
286 procedure has started, the respective canister fills a balloon independently. The right canister
287 module and the left canister module are independent systems. It realizes high observation
288 continuity by duplicating gas, air and electric systems. The canister module on one side can be
289 moved to the preparation room to load the sonde and facilitate the operator’s work. The new ARL
290 version can also recover from balloon bursts without human intervention at the site by using a
291 balloon from another canister. In the previous version, an operator had to visit the ARL to remove
292 broken balloons and restart the ARL during the observation window in such cases.

293 The new system is also equipped with a new simplified wind shield for launches in strong wind
294 conditions. All information and data are stored in a database available for each ARL. Various central
295 monitoring/control functions are provided by using application software and a web browser to
296 access the database on the workstation installed in the ARL. The Meisei ARL GC consists of a
297 temperature and humidity reference sensor and an inspection box. The GC performs before the
298 sonde loading. The results from the GC are not used in the data processing but only to check if there
299 are anomalies in the radiosondes.

300 In Table 3, the Meisei Automated Radiosonde System specifications are provided.

301 Figure 4 shows a photo of the system along with a sketch of the internals of system container. For
302 more details on the Meisei ARL experimental setup visit the Meisei website
303 (<http://www.meisei.jp/ars>). Japan Meteorological Agency (JMA) collects Meisei ARLs data since
304 2006. Parallel radiosoundings of auto launch and manual launch have not been done yet. This is the
305 reason why this paper does not show additional datasets or comparisons involving Meisei ARL: at
306 this stage, the description of the Meisei ARL is the only information which can be shared with
307 readers, according to recommendations provided by Meisei.



308

309

Table 3: Meisei ARS specifications

Dimensions	Width: 2.50 m
	Length: 6.20 m
Launch Tube Diameter	2.20 m x 1.80 m square
Height during transport	3.10 m
Total height with launcher tube	1.90 m (2.80 m including windshield)
Gross weight with launcher tube	6 t
Electrical energy consumption	< 1 kW (without air conditioning)

310

311

312 3. Technical performance

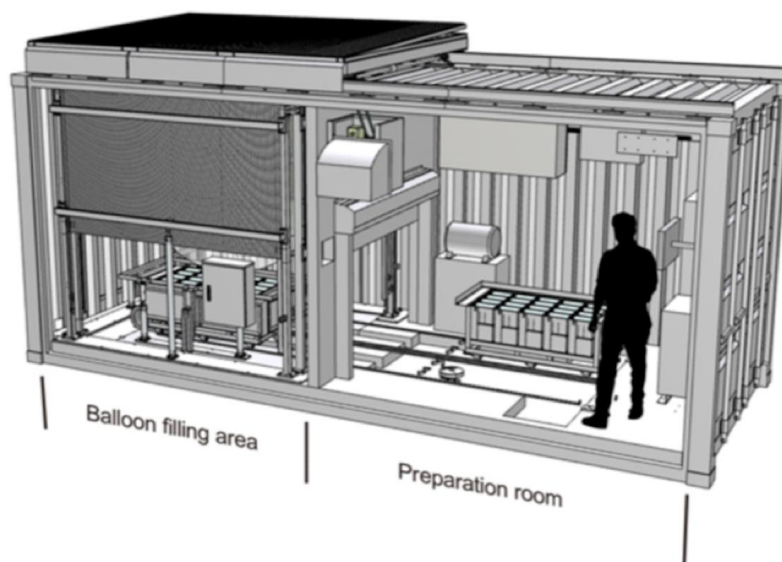
313

314 Beyond the automation of the radiosonde launch procedure, there are two main differences
315 between an ARL and a manual launch:

- 316 • Ground check procedures may be performed only during the sonde loading in the carousel
317 chamber, days or weeks before the sonde launch, though there is a trend towards less
318 frequent stocking;
- 319 • The use of independent and traceable calibration standards like the Standard Humidity
320 Chamber (SHC) is possible but only before the launch loading (also in this case one or more
321 days before the launch).

322 Both these aspects will be discussed in the following sections which provide potential technical
323 solutions to address the gaps between manual and automatic launch procedures in terms of
324 performance and traceability.

325



326

327 Figure 4: Picture of a Meisei Automatic Balloon Launcher (top panel) and sketch of the internals of ARL container in its
328 most updated configuration (bottom panel).

329

330 This section instead aims to provide a classification of the main challenges met by the stations which
331 have operated ARLs over several years and to assess the technical performance of the ARLs
332 compared to manual launches. The section is built upon the feedback provided by the GRUAN sites
333 in response to a survey for the collection of ARL information. Most of the ARLs at GRUAN sites are
334 from Vaisala (thus the analysis is not representative of Meisei and Meteomodem systems due to
335 the very limited feedback available for these systems). Given the small sample size, this is presented



336 qualitatively rather than quantitatively and it is anonymised. Examples of technical performance in
337 the field are then provided for a Vaisala and a Meteomodem ARL operating the most recent updated
338 version of the respective manufactured systems (at Payerne and Trappes stations).

339 A conceptual diagram to represent a generic ARL is provided in Figure 5: each ARL can be
340 schematically divided into 4 areas as follows:

- 341 ● the operator's area, where the operators can manage the system, prepare radiosondes and
342 balloons to be uploaded and where the station reception and processing units are located;
- 343 ● the ready-to-launch sondes storage area, built around the ARL rotating trays, where most
344 of the automated technologies are implemented to allow a completely unmanned launch;
- 345 ● the launching vessel area, where the balloon is filled and becomes ready for the launch;
- 346 ● external area, where all the ancillary instruments, such as the weather station and GNSS
347 antenna, are located along with gas tanks.

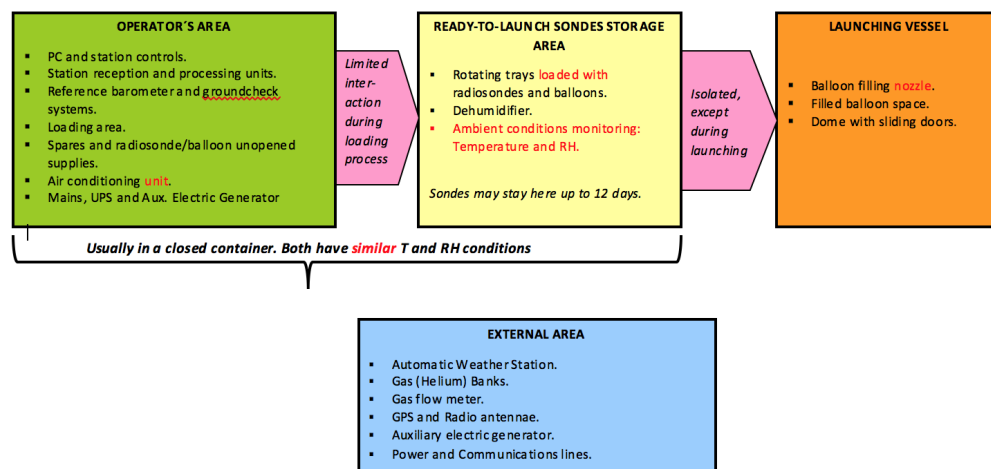
348 For each area, the weakest points identified from the GRUAN sites operating an ARL are:

- 349 ● in the operator's area, most of the issues are related to the not infrequent failure of power
350 supply system or of the air conditioning system, often related to a major failure of the power
351 supply at the measurement station itself; this anyhow represents a weakness in the use of
352 ARLs in remote areas, where logically the ARL might be an obvious choice; a few sites also
353 reported issues in the software and logic controllers;
- 354 ● the ready-to-launch sonde storage area is surely the most efficient part of ARLs, where few
355 issues are reported which indicates the robustness of these areas; the most critical issue
356 identified in this area is the infrequent failure of the air compressor;
- 357 ● the launching vessel area is where the balloon is filled and launched and where, therefore,
358 we have a high exposure to many environmental factors like harsh climate, dust, animals,
359 etc., which can strongly affect a successful launch also with later effects to the balloon and
360 early burst; several issues are raised by the stations related to challenges in the balloon
361 inflation process, failure of balloon presence sensor allowing launch of under-inflated
362 balloons, gas tubes bent and frozen gas hoses, balloon blocked on the tray, failure of the
363 rams which open vessel cover doors (this concerns Vaisala or Meisei, and not Meteomodem
364 ARL), delays in launch detection time compared to the actual launch time, occasional break
365 of the radiosonde string at launch (for Meisei);
- 366 ● the external area, is another critical area where several problems have been reported about
367 the gas flow meter and the switching between the gas tanks (one close to empty and the



368 other fully filled); extreme weather conditions (e.g very strong winds) can make the launch
369 more difficult, despite the additional screens protecting the balloon flight in the first 2-3
370 meters above the ARL (only for Vaisala and Meisei).
371 The problems listed above are not common to all the ARLs, each system has its own specific issues.
372 On one side, the feedback reported from GRUAN stations can provide a first assessment of the
373 challenges in operating an ARL: this study cannot assess challenges in the operation of each specific
374 model and it cannot quantify the improvements of each ARL with the time. The issues discussed
375 above could be used as recommendations to the manufacturers to foster further improvements of
376 the systems. The ARLs are typically maintained by the manufacturers on an annual check up
377 (performed remotely) and major maintenance approximately every 3 years. This maintenance
378 schedule, if applied at each station can increase the reliability of the systems over short and long
379 term, although it generates a cost increase.

380



381
382
383
384
385

Figure 5: Conceptual diagram of a typical automatic radiosonde launcher divided in four main areas: operator's area (green), ready-to-launch sondes storage area (yellow), launching vessel area (orange) and external area (cyan).

386 To assess the effective technical performances of the ARL launches vs manual launches, in Table 4
387 and 5, examples of the statistics collected at two GRUAN sites running an ARL, Payerne (WIGOS
388 station identifier=0-20000-0-06610, 46.82N, 6.93E, 490m asl), operated by MeteoSwiss, and
389 Trappes, operated by Meteo France, respectively, are reported. The Table provides a summary of
390 pertinent characteristics of the ARL versus manual launches. For Payerne, statistics are related only
391 to the automatic and manual launches performed since April 2018 (on average, ARL nine per week,
392 manual five per week) using the Vaisala AS15 ARL. For Trappes, manual launches were performed



393 in the period 2012-2014, while the Meteomodem Robotsonde has been operated in the period
394 2016-2018; in both cases two launches per day were performed with similar daily scheduling.
395 At Payerne, since April 2018 the Vaisala ARL has realized 470 successful flights per year, while
396 manual launches have been 260 per year. Effective flights according to MeteoSwiss standards are
397 launches with a balloon burst higher than 100 hPa with no telemetry lost or sensor failure. Despite
398 the use of different balloon sizes due to the fact that for manual launches bigger balloons are often
399 used to perform ozonesoundings, the percentage of successful launches as well the percentage of
400 sondes reaching 10 hPa pressure level is indistinguishable between the ARL and the manual
401 launches, with a limited use of spare sondes due to the failure of scheduled launches (4 %). Ascent
402 speed statistics are very close with better performance of the ARL in preventing very low balloon
403 gas filling.

404 At Trappes station (Table 5), during the period January 2016 to December 2018, the Meteomodem
405 ARL Robotsonde in Trappes has realized 1908 successful flights, out of a total of 1956 successful
406 flights according to MeteoFrance standards (balloon burst at pressure lower than 150 hPa with no
407 telemetry lost or sensor failure). The mean percentage of successful launches is 97.9% (2016: 95.5%,
408 2017: 98.2%, 2018: 99.1%, 2019(Jan-Oct): 98.6%, see Figure 6) with an evident improvement using
409 ARL in the percentage of sondes reaching 10 hPa pressure level (80%) compared to the manual
410 launches (60 %). The use of Totex balloons is one of the reasons for the improvement and further
411 improvement was achieved by increasing the size of the balloon. Moreover, since November 2016
412 Meteomodem has installed a flexible cover which assures that during the storage the balloon is less
413 exposed to contact with the air-conditioned environment. This seems to reduce the effects of drier
414 air on the balloon and improve its performance in terms of burst altitude (standard deviation of
415 burst altitude is reduced after the installation of the cover – not shown). For the balloon ascent
416 speed, comparison statistics between ARL and manual launches show also similar results.

417 According to the information shared by Meteomodem, it is also possible to add that, compared to
418 all the ARLs operated at other sites during the same period reported in Table 5, the Trappes ARL has
419 typically the same failure statistics. The time evolution of the failure (Figure 6) shows that the
420 number of spares and the number of failures by type halved in three years to reach less than 2%
421 relative to the number of successful flights. For the 578 flights performed during 2018, the absolute
422 number of failures is 2 to the ARL (which was a radio loss and an inflation problem), 1 failure due to
423 sensor break, no failure from the software, 1 failure which is not classified by our automated failure



424 identification and 1 failure due to the use of ARL which can be an operator stop or an obstructed
425 inflation tube.

426

427

428 Table 4: Technical performance of automatic vs manual launches performed at Payerne station
429 during 2018 for a Vaisala AS15 ARL. Metadata related to the sonde and balloon types are shown
430 alongside the percentage of success for the launches performed during the reported period, the
431 percentage of spare sondes used, the sondes bursting before reaching 10 hPa, and the maximum,
432 minimum and average ascent speed.

433

434

Station	Automatic	Manual
Station type	AS15	MW41
RS type	RS41	RS41 (+ ECC ozonesonde)
Balloon type	Totex	Totex
Balloon size	800g	800g/1200g/2000g/3000g
Number of launches	470/year	260/year
Percentage of successful flights	>99%	>99%
Percentage of spare	4%(spare if P>100hPa)	N/A
Sondes above 10 hPa	92% (based on 2018)	92% (based on 2018)
Max. Ascent speed	6.1 m/s	6 m/s
Min. Ascent speed	3.5 m/s	3 m/s
Avg. Ascent speed	5.2m/s	5m/s

435

436

437

438

439

440

441

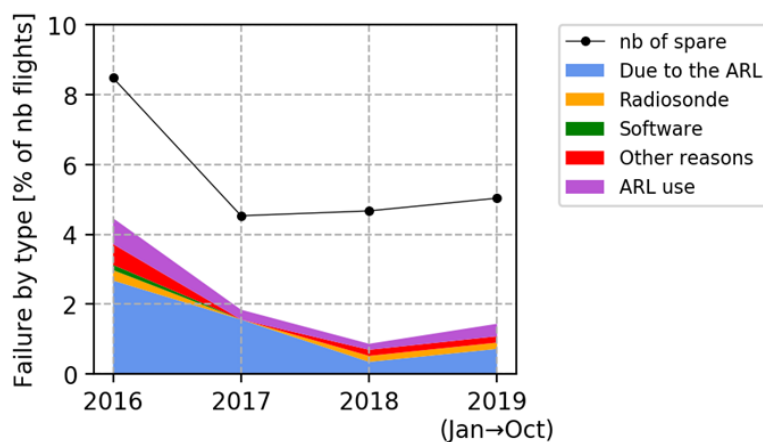
442



443 Table 5: Same as Table 4 for Trappes site in the period 2016-2018 and 2012-2014, respectively for a
 444 Meteomodem ARL.
 445

Station	Automatic	Manual
Station type	Robotsonde (14/04/2015 to 12/2018)	SR10 (01/01/2012 to 14/04/2015)
RStype	M10	M10
Balloon type	Totex	Hwoyee
Balloon size	350g/1000g	Hwoyee 600g
Number of launches	2106	2113
Percentage of successful flights	99% (based on 2018)	>99% (based on 2012)
Percentage of spare	5% (based on 2018)	N/A
Sondes above 10 hPa	80%	60%
Max. Ascent speed	6 m/s	6 m/s
Min. Ascent speed	4 m/s	4 m/s
Avg. Ascent speed	5 m/s	5.4 m/s

446



447

448 Figure 6: Cause of failure for the Meteomodem ARL in Trappes as a function of time since the
 449 installation date.



450

451 **4. Stability, ground calibration**

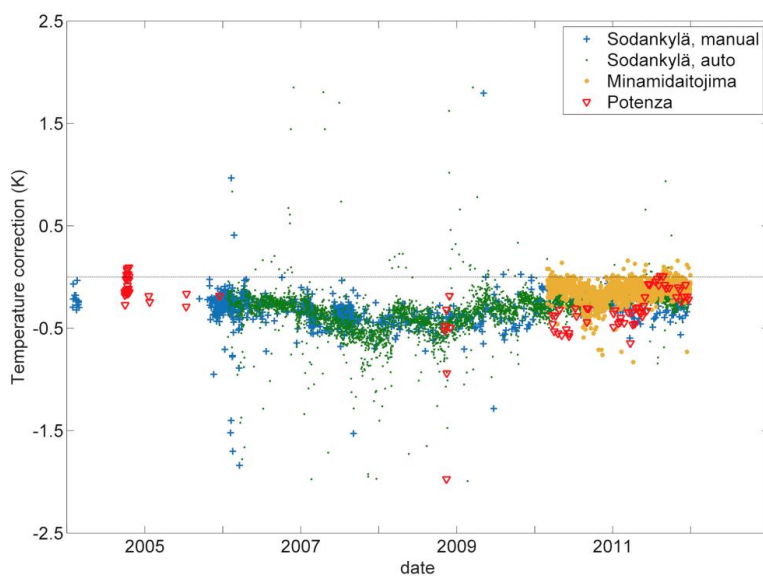
452 **4.1. Performance of the Vaisala ARL**

453 The performance of the Vaisala ARL has been evaluated through the analysis of a dataset collected
454 at Sodankylä station. The Sodankylä Vaisala ARL was used to regularly launch RS92 radiosondes at
455 11:30 and 23:30 UTC over 2006 to 2012. Manual soundings were periodically performed in parallel
456 using a similar Vaisala DigiCora-3 sounding system throughout this period. Parallel soundings have
457 been selected with launch time difference between 2 minutes and 20 minutes. A total of 283 parallel
458 soundings has been considered: these are distributed evenly across the period, with the exception
459 of 2006, which has more parallel soundings than other years, and most of these are daytime
460 comparisons. In addition, two Vaisala ARL datasets from the Potenza GRUAN station (40.60N,
461 15.72E, 760 m a.s.l.) and the Minamidaitojima station, run by JMA (WIGOS station identifier
462 index=0-20000-0-47945, 25.79N, 131.22E, 15 m a.s.l.), covering a similar time period, though much
463 smaller sample sizes than in Sodankylä, have been used for comparison. Despite the less intensive
464 sampling, Potenza and Minamidaitojima data are useful data sources to compare with Sodankylä
465 and, specifically, to check consistency of the GC correction across different stations and different
466 batches of Vaisala sondes.

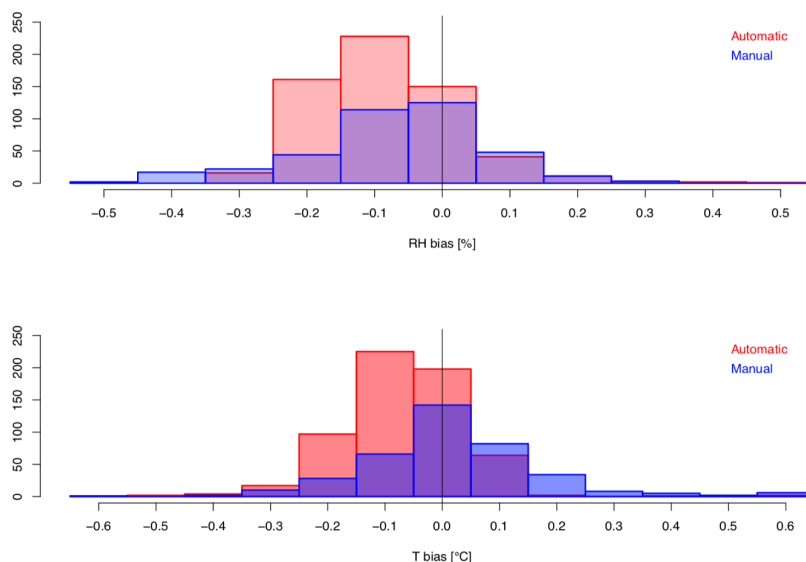
467 The availability of long time series of parallel sounding for the Sodankylä station permits
468 investigation of the system performance also in the pre-launch phase. Two main aspects are
469 evaluated: stability of the ground check correction on temperature, and potential effects related to
470 the time periods the sondes were stored before launch.

471 Figure 7 summarises the temperature correction applied during the GC procedure for the RS92
472 sondes of the above described data sets using the Vaisala GC25 ground check device, with most of
473 the launches performed since 2006. Figure 7 shows similar GC values at Sodankylä, Potenza and
474 Minamidaitojima stations despite the very different locations and launch scheduling, with a
475 negative adjustment of between smaller than -0.5 K before 2010 and smaller than -0.3 K typically
476 applied to most of the RS92 sondes with an improvement of the differences over the time in the
477 batches launched after 2009. The results shown in Figure 7 assume that all the reported ARL GC
478 temperature sensors were maintained according to recommendations described in the previous
479 section.

480



481
482 Figure 7: Time series of the temperature correction (temperature measured by the GC reference sensor minus
483 temperature measured by the sonde) applied during the GC procedure for the RS92 sondes launched at Sodankylä, both
484 manually (blue crosses) and automatically (green dots), and at Minamidaitojima (yellow dots) and Potenza (red
485 triangles, automatically) from 2004 to 2012.
486



487
488 Figure 8: Distribution of temperature and relative humidity corrections found during Vaisala GC process for the
489 automatic and the manual soundings operated at Payerne station using the RS41 radiosonde.
490

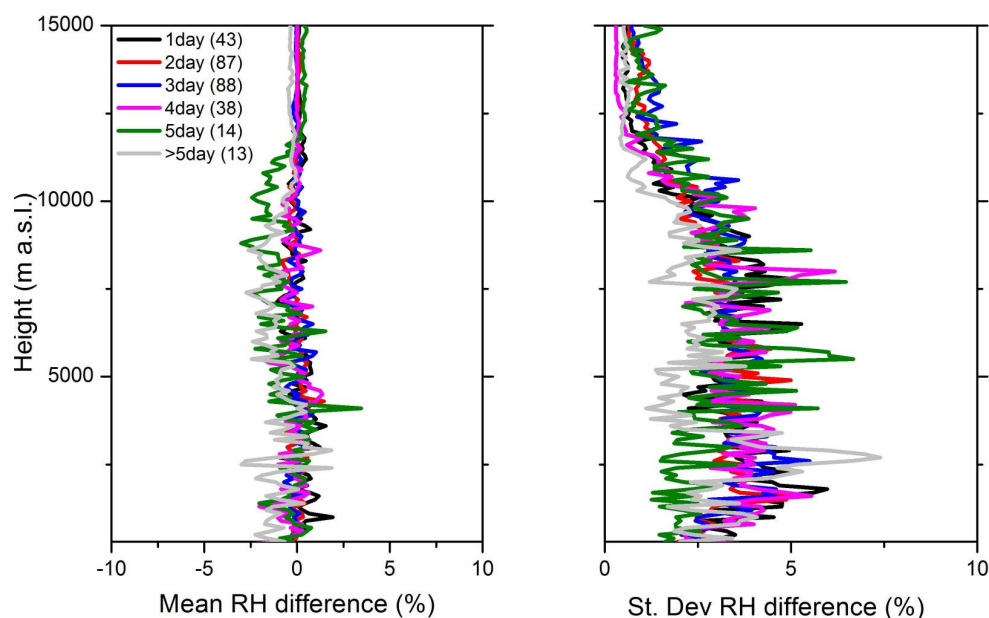


491 Results similar to those from Sodankylä and Potenza GRUAN stations are reported by Payerne
492 GRUAN station (Figure 8) using the RS41 since April 2018 and operating the Vaisala AS15 ARL. Figure
493 8 shows that the distribution of temperature and relative humidity corrections have negative
494 skewness with the GC adjustments within a few tenths of a degree and the average adjustment is
495 smaller than 0.1 K and 0.1% RH, respectively. These results show an average negative GC corrections
496 for the ARL in analogy to the results reported above for RS92 sondes at Sodankylä and Potenza,
497 where also the old Vaisala ARL version was operated. Comparisons with the broader statistics
498 collected by for GRUAN station launching manually (not shown) reveal results consistent with the
499 GC time series shown in Figure 7 and 8, thus excluding the presence of clear systematic effects in
500 the GC corrections due to the use of ARLs. Nevertheless, the small differences observed between
501 the ARL and manual GC corrections needs further investigations to understand if performing the GC
502 in a controlled temperature and humidity environment may generally improve or worsen the
503 calibration in the long term.

504 In an operational station like Sodankylä, the time between balloon loading and ground check can
505 vary from day to day. At Sodankylä average loading time was 2-3 days prior to launch for regular
506 soundings. The ARL software allows also longer times in the tray. Figure 9 shows the mean
507 differences of simultaneous RH profiles (left panel) measured using the ARL and the manual
508 soundings as a function of the number of days a sonde stays on a tray before launch, from 1 to more
509 than 5 days. The corresponding standard deviations are also shown (right panel), while in brackets
510 within the color legend, the number of parallel soundings for each time period is reported. To
511 calculate the statistics shown in section 4 and 5, radiosounding temperature and RH from parallel
512 soundings have been interpolated to a 100-meter vertical grid. Figure 9 shows that there are no RH
513 systematic differences when parallel launches are grouped according to the tray time, except for
514 the launches with a tray time of 5 days or more at altitude levels above 7 km a.g.l., where a mean
515 difference smaller than -2.0 % RH is obtained up to 10-12 km a.g.l. Nevertheless, it must be noted
516 that the size of the sample investigated for these tray time options (5 days and >5 days) is much
517 smaller than for other tray times and these launches include also parallel sounding with longer
518 differences in the respective balloon release time. A Wilcoxon Rank Sum Test has been applied and
519 the computed probability ranges within 0.4-0.5 with smaller values only for above 12 km a.g.l., where
520 the probability becomes larger than 0.2. For the time tray option with a smaller sample of parallel
521 soundings (1 day, 5 day and >5 days), the probability oscillates between 0.05 and 0.10. Therefore,
522 it is possible to conclude that we do not reject the hypothesis that the two data distributions (ARL



523 and manual launches) have the same median value and the reported comparisons are meaningful.
524 Finally, the right panel of Figure 4 show that the standard deviations are substantially smaller than
525 5% RH at all altitude levels without any evident correlation with tray time. A similar test for longer
526 storage time, up to one month, has been carried out recently in Sodankylä providing similar GC
527 results (not shown).

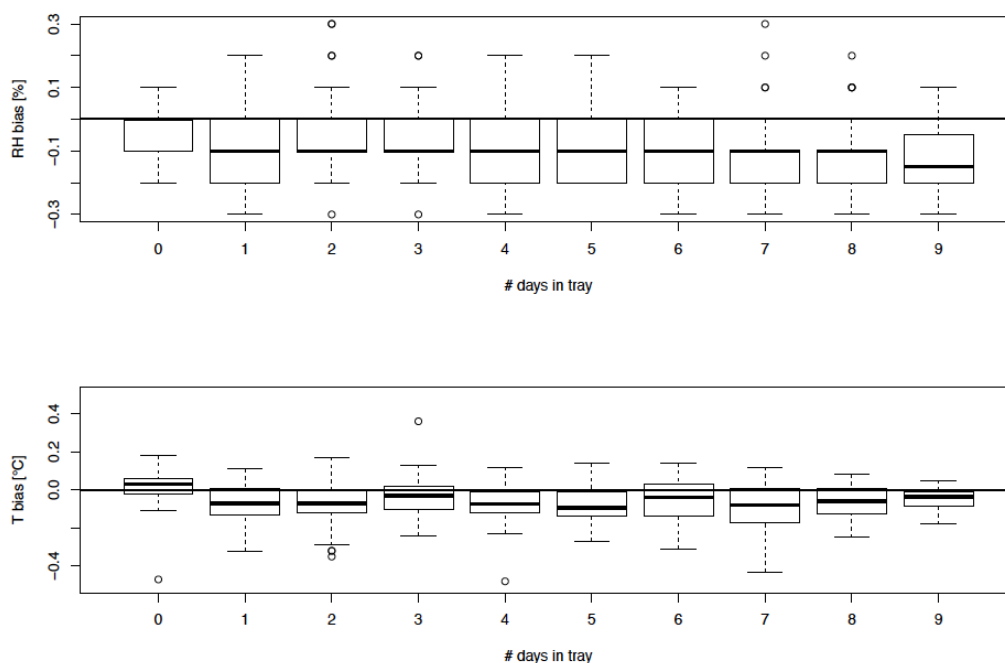


528
529 Figure 9: Vertical profiles of the mean difference and standard deviation of the RH measured with the manual and
530 automatic system in Sodankylä as a function of the time period between GC and launch; from left to the right, the time
531 period increases from 1 to more than 5 days. In brackets within the legend, the number of parallel soundings considered
532 for each time period is reported.
533

534 In Figure 10, a similar study to that reported in Figure 9 is presented for the Payerne station. In this
535 case, the average difference and the standard deviation of temperature and relative humidity found
536 during the GC using Vaisala RS41 radiosondes into the Vaisala AS15 versus the aging (up to 9 days
537 into tray from the loading until launch) is shown. For both temperature and relative humidity,
538 excluding only the launches which occurred within 24 hours of the radiosonde loading, the bias is
539 negative and independent of any further aging. Until one day after loading the bias is stable close
540 to zero and thereafter it increases to about -0.1 K and -0.1% over the following days. These results
541 show how the use of ARLs also in remote places or where it is required to upload in advance a large
542 number of radiosondes, to launch with a few days of delay, do not appreciably lead to changes in
543 the Vaisala GC.



544 In Figure 10, a similar study to that reported in Figure 9 is presented for the Payerne station. In this
545 case, the average difference and the standard deviation of temperature and relative humidity found
546 during the GC using Vaisala RS41 radiosondes into the Vaisala AS15 versus the aging (up to 9 days
547 into tray from the loading until launch) is shown. For both temperature and relative humidity,
548 excluding only the launches which occurred within 24 hours of the radiosonde loading, the bias is
549 negative and independent of any further aging. Until one day after loading the bias is stable close
550 to zero and thereafter it increases to about -0.1 K and -0.1% over the following days. These results
551 show how the use of ARLs also in remote places or where it is required to upload in advance a large
552 number of radiosondes, to launch with a few days of delay, do not appreciably lead to changes in
553 the Vaisala GC.
554



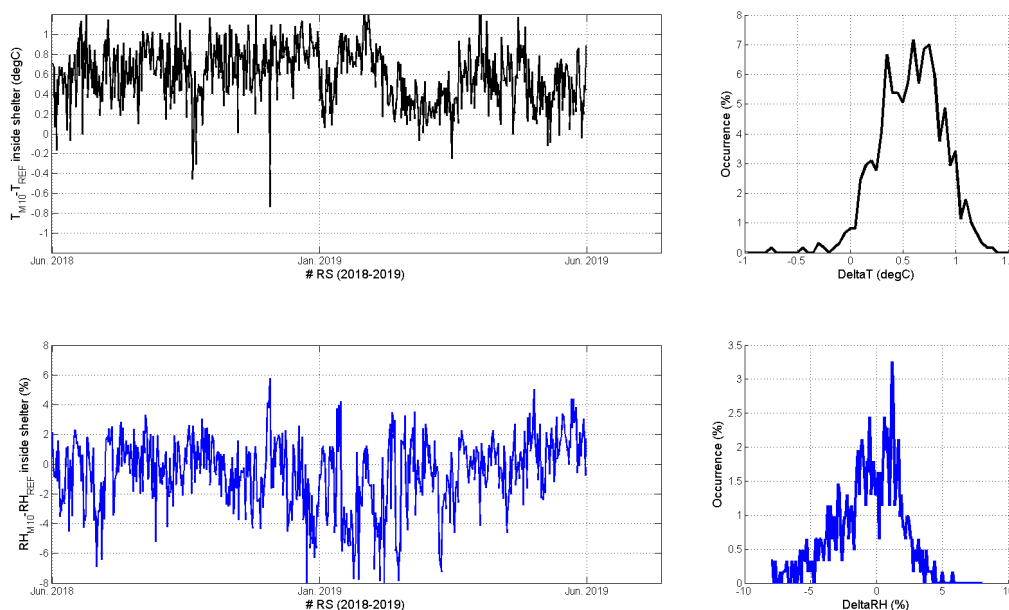
555
556 Figure 10: Average difference and standard deviation of temperature and relative humidity found during the Vaisala GC
557 process versus the aging (number of days into tray from the loading until launch) of the radiosonde RS41 into the
558 Payerne ARL (Vaisala AS15).
559

560 4.2. Performance of the Meteomodem ARL

561 The performance of the Meteomodem ARL ground-check has been evaluated through the analysis
562 of a dataset collected at MétéoFrance Trappes station, where M10 radiosondes have been launched
563 regularly at 11:30 and 23:30 UTC since 2016. The availability of a long time series for the comparison



564 between M10 temperature and humidity sensor and one reference temperature/humidity sensor
565 (Vaisala HMP110, [https://www.vaisala.com/sites/default/files/documents/HMP110-Datasheet-](https://www.vaisala.com/sites/default/files/documents/HMP110-Datasheet-B210852EN_1.pdf)
566 [B210852EN_1.pdf](https://www.vaisala.com/sites/default/files/documents/HMP110-Datasheet-B210852EN_1.pdf)) at ambient conditions, inside a meteorological shelter for the Trappes station,
567 permits the investigation of the system performance also in the pre-launch phase. Since June 2018,
568 this comparison is carried out during the 5 minutes before each automatic sounding. Figure 11
569 summarizes the time series and PDF of the difference between M10 and HMP110 sensor for
570 temperature (black curve, upper panel) and relative humidity (blue curve, lower panel) recorded
571 between June 2018 and June 2019. The relative humidity difference oscillates around 0% and in
572 more than 75% of the cases the difference is smaller than 2% RH in absolute value. For temperature,
573 the observed residual difference around 0.5°C requires further investigations.
574



575
576 Figure 11: Time series and pdf of the difference between M10 and HMP110 sensor for temperature (black curve) and
577 relative humidity (blue curve) between June 2018 and June 2019, measured at ground level inside a meteorological
578 shelter in ambient condition.
579

580 Figure 12 provides a picture of the meteorological shelter and the position of the HMP110 and the
581 M10 during the 5-minutes comparison shown in Figure 11. These results need further investigations
582 in order to determine if the systematic difference observed on temperature in the meteorological
583 shelter is due to the Meteomodem M10 batches produced in 2018, though Meteomodem did not
584 report similar systematic difference during the production checks, or if this could be due to the need



585 of improving in the experimental protocol. The meteorological shelter has been improved with the
586 installation of a fan (Figure 12) which should produce a better homogenisation of the temperature
587 and relative humidity around the two sensors. The development of a new experimental protocol is
588 under consideration and should lead to the production of a tube ventilated by a laminar flow in
589 which the Meteomodem M10 and a PTU reference could measure under the same environment,
590 upon the characterization of the spatial homogeneity of the temperature and relative humidity.
591



592
593 Figure 12: Picture of the meteorological shelter in Trappes (left panel: general view: the meteorological is near the
594 Meteomodem ARL entrance for simplicity reasons, right panel: inside of the meteorological shelter)

595
596 Finally, the M10 radiosonde is put inside a SHC chamber for 3 minutes before the sounding (with a
597 relative humidity near 100%): more than 95% of the samplings are accepted after the test. For
598 operational reasons, the Meteomodem probes used in the GRUAN protocol, are tested in the
599 meteorological shelter and in the 100% RH test but not necessarily in this order at each time. It is
600 not known if the order of the checks makes any difference.

601

602 5. Vertical velocity and balloon burst

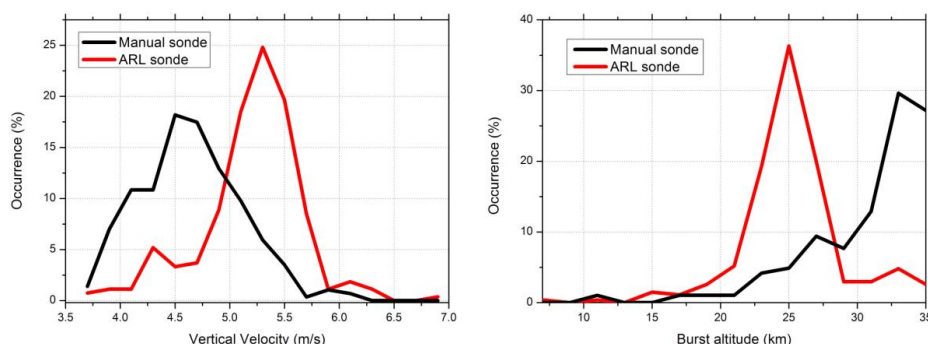
603 This section reports the statistics for the vertical velocity and the balloon burst altitudes from the
604 datasets collected at Sodankylä and Trappes stations.



605 **5.1 Vertical velocity and balloon burst altitude for Vaisala technology**

606 In Figure 13, the statistics of the balloon vertical velocity and of the burst altitude for Sodankylä in
607 the period from 2006 to 2012 are shown. In terms of vertical velocity (Figure 13, left panel), the ARL
608 has a quasi-symmetric frequency distribution peaked around 5.3 m s^{-1} with a spread mainly between
609 4.7 m s^{-1} and 5.9 m s^{-1} . For the manual launches, the frequency distribution is quite wide, non-
610 symmetric, peaked around 4.5 m s^{-1} with a larger spread of the values mainly between 3.5 m s^{-1} and
611 5.7 m s^{-1} . The comparison reveals the higher stability of the ARL compared to manual launches in
612 controlling the balloon filling and, therefore, the sounding vertical velocity which is relevant for the
613 quality of the measured profile. For the balloon burst altitude (Figure 13, right panel), a real
614 comparison between the manual launches and the ARL is not feasible at Sodankylä due to the use
615 of different balloon types (typically smaller for the ARL) which causes a strong difference in balloon
616 altitude. Totex Tx800 or Tx600 type of balloons were used in winter and Totex Ta350 or Tx350 type
617 sounding balloons were flown during all other seasons. Due to smaller balloon volume, the
618 summertime soundings had lower burst heights on average. The burst altitude for the ARL has also
619 in this case a quasi-symmetric frequency distribution peaked around 25 km of altitude a.g.l. with a
620 spread of the values mainly between 17 km and 28 km a.g.l., while the distribution for manual
621 launches is non-symmetric, with a maximum frequency around 33 km and most of values ranging
622 within 21 - 35 km a.g.l. It must be mentioned that the differences between night-time and day-time
623 soundings were not significant, although night time soundings have on average lower burst heights
624 during polar vortex overhead conditions in winter.

625



626
627

628 Figure 13: Vertical velocity (left panel) for radiosondes launched manually (black line) and automatically (red line), along
629 with burst altitude (right panel) at Sodankylä station.

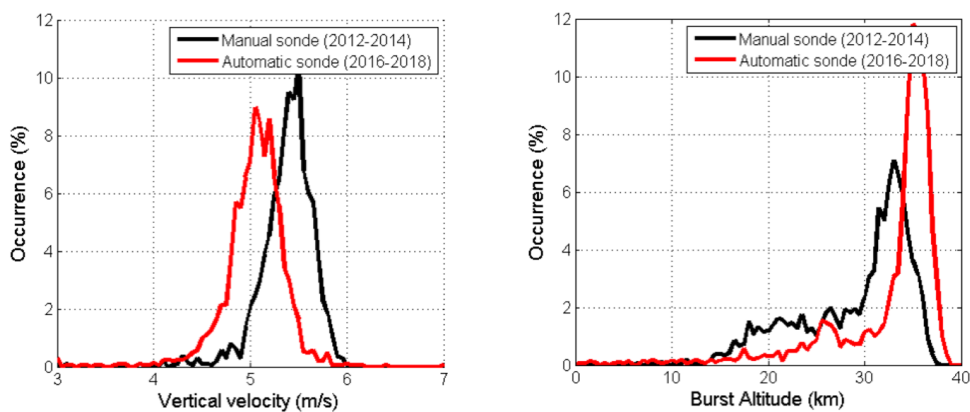
630



631 **5.2 Vertical velocity and balloon burst altitude for Meteomodem technology**

632 A more interesting comparison to show the positive influence of automation on the burst altitude
633 is those related to the dataset discussed in Section 3 and summarized in Table 5, shared by Meteo
634 France for Trappes station (Figure 14). In terms of vertical velocity (Figure 14, left panel), both the
635 ARL and the manual launches have a quasi-symmetric frequency distribution peaked around 5.5 m
636 s⁻¹ and 5.1 m s⁻¹, respectively, with a similar spread of about 1.0 m s⁻¹. For the burst altitude (Figure
637 14, right panel), we have for both the dataset a negatively skewed distribution with an evident peak
638 around 33 km for the manual launches and 35 km for the ARL. The comparison reveals that the burst
639 altitude (Figure 14, right panel) is significantly higher and less scattered after the automation, while
640 the vertical velocity of the balloon has not significantly changed (Figure 14, left panel). 40 % of the
641 balloons burst before 30 km during the manual period, where only 20 % during the automatic
642 period, this result means that the Meteomodem ARL and/or the operational organization has
643 increased by a factor two the number of balloons reaching an altitude higher than 30 km. The burst
644 altitude for both periods (2012-2014 for the manual launches and 2016-2018 for the ARL) shows
645 some seasonal signal. It appears that burst altitude is lower during the winter. A further study could
646 evaluate burst altitude as a function of air temperature or potential vorticity in order to study the
647 influence of polar vortex and its potential impact on the burst altitude.

648
649



650
651
652
653
654
655

Figure 14: Vertical velocity (left panel) for radiosondes launched manually (black line) and automatically (red line), along with burst altitude (right panel) at Trappes station.



656 **5.3 Quantifying relative performance**

657 In this section, two datasets are investigated to assess the differences in the vertical profiles of
658 temperature and humidity: the set of RS-92 parallel (automatic and manual) soundings performed
659 with the automatic radiosonde launchers at Sodankylä along with a second set of Meteomodem
660 radiosoundings collected at Faa'a station, French Polynesia. In the following analysis, given the
661 latitude ϕ , the longitude λ , the Earth's radius R (mean radius = 6371 km), the distance between two
662 balloons (1 and 2) has been calculated using the 'haversine' formula (Sheppard and Soule, 1922)
663 which provides the great-circle distance between two points (i.e., shortest distance over the earth's
664 surface):

$$665 \quad d = Rc$$

666 where

$$667 \quad c = 2 \operatorname{atan2}(\sqrt{a}, \sqrt{1-a})$$

668

$$669 \quad a = \sin^2\left(\frac{\Delta\lambda}{2}\right) + \cos(\varphi_1) \cos(\varphi_2) \sin^2\left(\frac{\Delta\lambda}{2}\right)$$

670

671 The haversine formula remains particularly well-conditioned for numerical computation even at
672 small distances – unlike calculations based on the spherical law of cosines. The function “atan2” is
673 described in Glisson (2011).

674 The two datasets are also investigated to show the correlation between the difference in the vertical
675 profiles and the distance between the two flying sondes.

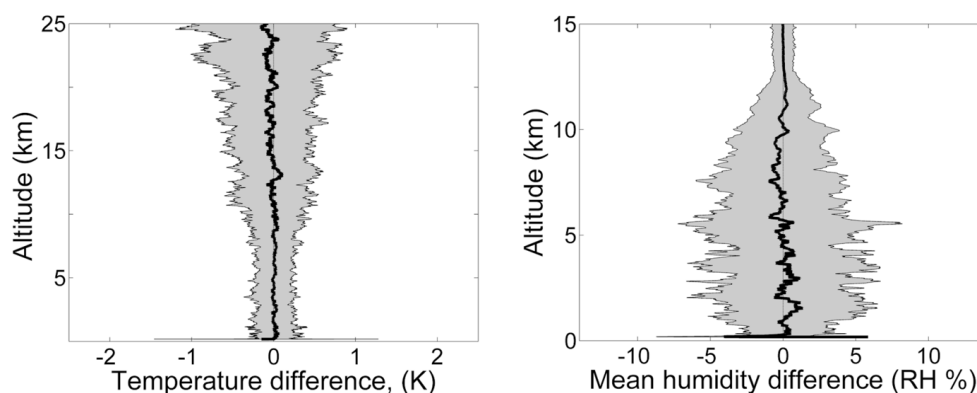
676

677 **5.1 Parallel soundings with Vaisala systems**

678 For the same six-year dataset collected at Sodankylä discussed in Section 4, the vertical profiles of
679 the average differences (automatic minus manual) and standard deviations of the temperature and
680 RH measured during parallel soundings are shown in the left panel of Figure 15. Systematic
681 differences in the temperature profile are negligible (on average smaller than 0.01 K) over the entire
682 vertical range up to 25 km a.g.l, while the standard deviation increases with altitude from values
683 smaller than ± 0.5 K below 15 km to values larger than 1 K above. The result is in agreement with the
684 increase in mean distance between near simultaneous sonde paths at higher altitudes (Figure 16).
685 A subset of the parallel temperature soundings at Sodankylä has previously been analyzed by
686 Sofieva et al. (2008). Even though it is hard to separate components from non-collocation from those
687 which may arise from instrument-to-instrument differences (e.g. arising from manufacture
688 variations and differences in preparation, storage and launch at the uppermost altitudes), Sofieva

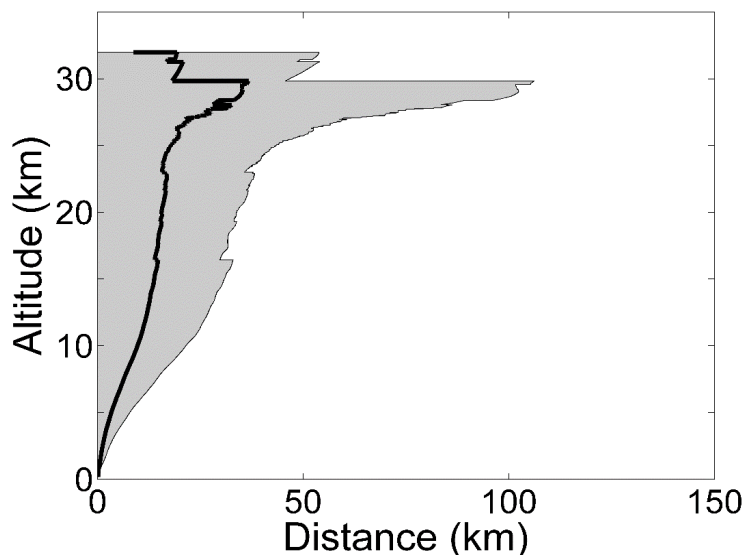


689 et al. found differences in small scale structures in temperature profiles, when the horizontal
690 separation was larger than 20 km. Moreover, to investigate whether the ARL and the manual
691 radiosoundings datasets were selected from populations having the same distribution, i.e. if the
692 calculated mean differences are statistically significant, the Wilcoxon Rank Sum test has been
693 applied: this confirm that the two datasets are samples of the same population showing a
694 probability larger than 0.5 for temperature at all the altitude levels below 20 km and values larger
695 than 0.1 above, while for RH values larger than 0.3 over the entire range from surface to 15 km a.g.l



696

697 Figure 15: Temperature (left panel) and RH (right panel) mean difference between ARL and manual for the six-year
698 dataset of parallel soundings collected at Sodankylä station at all altitude levels up to 25 km a.g.l for temperature and
699 up to 15 km a.g.l for RH. Standard deviation at each pressure level is reported using the gray area.
700



701

702 Figure 16: Horizontal distance between the balloons calculated for the six-year dataset of parallel soundings collected
703 at Sodankylä station for all the altitude levels up to 32 km a.g.l.



704 For the RH mean difference profile (Figure 15, right panel), there are no significant systematic
705 differences up to 7 km and then again above 10 km a.g.l., while in between these altitudes a small
706 negative mean difference lower than 1% RH is found and may be related to the coupling between
707 the RH variability in the upper troposphere and the distance between the two sondes. The increase
708 in standard deviation the lower troposphere below 5 km a.g.l., with values generally smaller than
709 5% RH, it is due to the high RH variability which can be significant even for small horizontal distances
710 between the two sondes. Above 5 km, going to the UT/LS where the values of RH are on average
711 smaller and less variable, RH difference decreases except when clouds or other uncommon events
712 are detected (e.g. Stratospheric-Tropospheric exchanges).

713 In addition, the analysis was rerun after grouping the ARL flights according to the time a sonde had
714 been loaded to the launcher system (see section 4): variations of time period between sonde loading
715 and actual launch time did not influence the comparison results.

716 Finally, the Wilcoxon Rank Sum Test has been applied to the entire dataset and the computed
717 probability that the two samples belong to the same population is larger than 0.35 at all altitude
718 levels.

719

720 **5.4 Parallel soundings at Faa'a with Meteomodem systems**

721 A first evaluation of the performance of Meteomodem ARL is provided by the analysis of the
722 datasets collected over 3-14 October 2018 at Faa'a station (French Polynesia, 28.34S, 16.32E, 21 m
723 a.s.l.) where 21 launches (9 day-time and 12 night-time) of parallel radiosoundings have been
724 undertaken (a picture is provided in Figure 17) in order both to compare temperature, relative
725 humidity, wind speed and direction, and to study further characteristics of the flights (burst altitude,
726 ascent speed for example). Meteo-France has conducted the Intensive Operational Period while
727 Institut Pierre Simon Laplace (IPSL) has produced the NetCDF files (data and metadata) for the
728 analysis. Raw data without any correction for temperature and relative humidity have been
729 considered in this paper. The GRUAN data processing, which remains under development at the
730 present time for this datastream, has not been applied. The manufacturer Meteomodem IR2010
731 software was used for both manual and automatic launches.

732 ECMWF noted that some reports from Meteomodem Robotsondes at other stations had
733 anomalously dry, and sometimes warm, values just above the surface relative to the background
734 field. In cool, moist atmospheric conditions the anomalies can be two or three degrees for
735 temperature and larger for dew point temperature. "For technical reasons the launcher has to be
736 kept warm and dry internally, which means that the humidity sensor is initially reading quite low



737 and a bubble of warm/dry air escapes with the balloon at launch - the net effect is that the first few
738 decametres the dewpoint reading is too low.” (Ray McGrath, pers. comm. 2015). The issue
739 described above does not affect the profile at higher levels. A similar issue has also been reported
740 for data taken during the first few seconds with Meisei ARL and this is suspected to be due again to
741 the influence of the air inside the launcher.
742



743
744 Figure 17: Daytime parallel sounding at Faa'a station (French Polynesia).
745

746 The Meteomodem has recently implemented a new software, EOSCAN, not yet implemented at all
747 the stations, which improves the ARL dataset quality with a number of corrections such as:

- 748 1. Eliminating the GPS disturbances at the end of the tube that can persist in the first 20 seconds
749 after the release;
- 750 2. Adjusting for the systematic bias introduced by the fact that the ARL Meteomodem is air
751 conditioned and affecting the first 150 m of the radiosounding profiles.

752 The dataset collected by Meteo-France at Faa'a station is not sufficiently large to draw robust
753 statistical inferences. Nevertheless, this dataset is the first ever available to evaluate the
754 performances of the Meteomodem ARL and can provide useful indications of any likely impact upon
755 the data quality of ARL facilities.

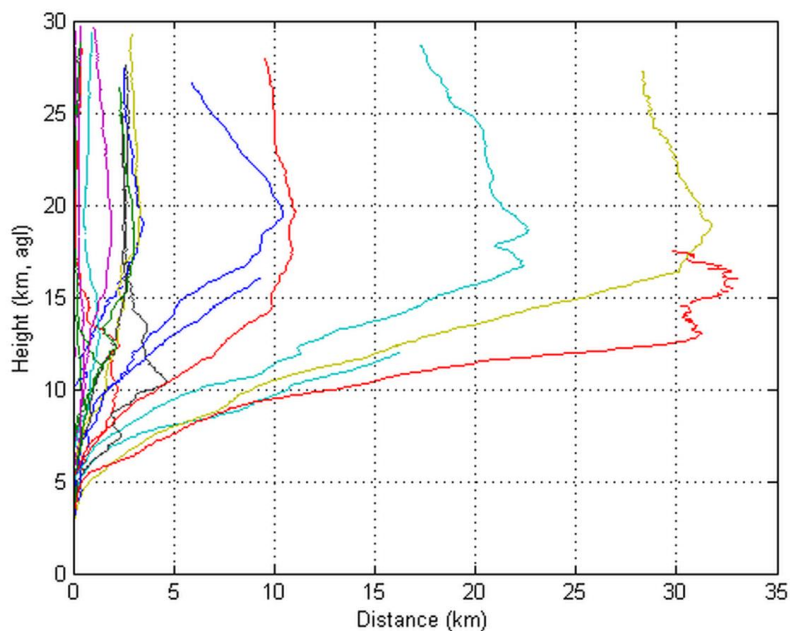
756 Before comparing, the T and RH profiles of the parallel sounding dataset have been interpolated to
757 a resolution of 100 m altitude. The difference between the launch time of the ARL and the manual
758 balloons ranges within 1 and 12 seconds.



759 In Figure 18, the horizontal distance between the pairs of parallel soundings at all the altitude level
760 up to 25 km a.g.l is shown: the horizontal distance between the two balloons is typically within
761 about 35 km.

762 In Figure 19, the difference between the balloon automatically released and the manual one as a
763 function of altitude regardless of time mismatch, for each pair of parallel soundings is reported
764 (black line) along with the corresponding mean difference (grey dashed line); the left panel shows
765 the difference for temperature, while the right panel for RH. The mean temperature difference is
766 smaller than ± 0.2 K up to 12-13 km a.g.l., and typically smaller than ± 0.5 K above. The difference is
767 negative, up to -2.0 K, in the first 50-100 meters and this is probably due to the potential warming
768 effect of the ARL environment on the radiosonde sensor.

769



770

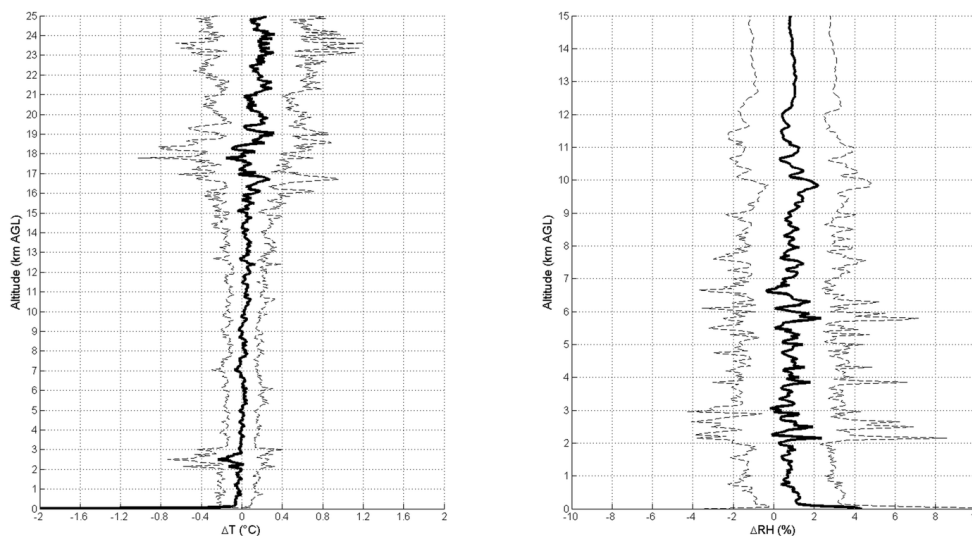
771 Figure 18: Horizontal distance calculated for the balloons of the 21 parallel soundings performed at Faa'a station for all
772 the altitude levels up to 25 km a.g.l. Measurement time between the two sondes at the same altitude levels may differ
773 and at the start time ranges within 1-12 seconds.

774

775 For RH, the mean difference is instead always positive and smaller than 0.7% RH up to 8 km a.g.l.
776 with a standard deviation smaller than 3-4% RH. Above 8 km, the mean difference becomes larger
777 and less variable with a maximum of about 2% RH and a standard deviation around 3%. The
778 Wilcoxon Rank rank sum test has been applied to both temperature and RH. For temperature, the



779 probability is higher than 0.3 until 17 km and higher than 0.2 above, while for RH is larger than 0.2
780 below 10 km and larger than 0.1 above. Only in the first 40 m for temperature and the first 20 m for
781 RH, the Wilcoxon Rank sum test fails with a probability lower than 0.05. The results of the test
782 allow to confirm the null hypothesis of the same median for the ARL and manual data distribution
783 at all the height levels for both temperature and RH, with the only exception of a few decameter
784 above the ground because of the ARL air conditioned effect. The reason behind this bias could arise
785 from GC effects or differences in the pre-launch procedures between the two systems affecting the
786 performance of one of the two launches in a quasi-systematic manner throughout the vertical
787 profile. This will be further investigated with the support of the manufacturer.
788 In terms of balloon burst altitude the ARL proved to be reliable both during the daytime with a burst
789 altitude ranging within 26688 - 31904 m above ground level (a.g.l.) versus values within 24970 -
790 30621 m a.g.l. calculated for the manual launches, while during nighttime the burst altitude ranges
791 within 27587 - 30790 m a.g.l. for the automatic launcher versus values within 27437 - 30139 m a.g.l.
792 for the manual launches. Applying the Wilcoxon Rank-Sum Test, the computed probability (0.05224)
793 is slightly greater than the 0.05 significance level and therefore we do not reject the hypothesis that
794 the two distributions of burst altitude values, for ARL and manual launches respectively, have the
795 same median value, indicating that ARL does lead to improvements in the balloon burst altitude.
796



797
798 Figure 19: Difference between ARL and manual profiles of temperature (left panel) and RH (right panel) for 21 parallel
799 soundings performed at Faa'a station up to 25 km a.g.l. for temperature and up to 15 km a.g.l. for relative humidity.
800 Black lines: mean differences, dashed lines: standard deviation.



801

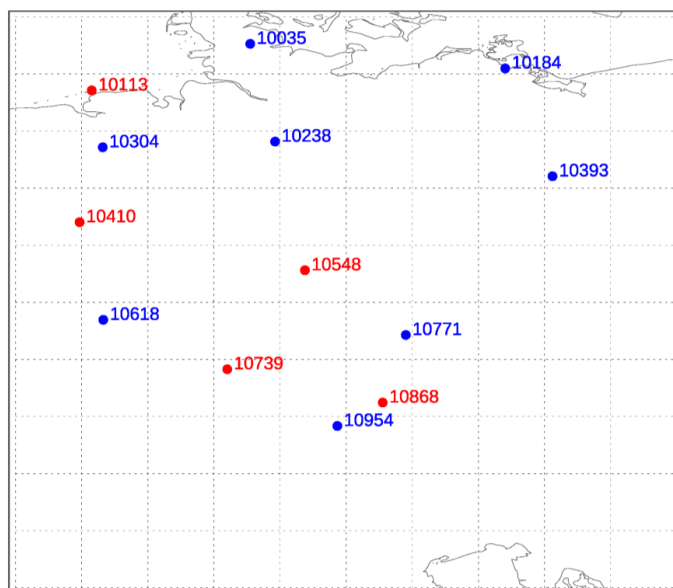
802 **6. Automatic launchers performance evaluated using the ECMWF forecast model**

803 Data assimilation systems compare observations with a short-range forecast (called the
804 background) and use observation-minus-background (O-B) differences in the assimilation to provide
805 improved initial conditions for the next forecast. For some areas/variables the uncertainties in the
806 background are now similar to, or smaller than, those in the observations, so the background
807 provides a very useful comparator. O-B differences from reanalyses have been also used to
808 homogenise historical radiosonde data (Haimberger et al., 2012). Ingleby (2017) compared different
809 radiosonde types with ECMWF background fields and for temperature and upper-tropospheric
810 humidity found differences in radiosonde performance that are broadly consistent with the results
811 of the last WMO radiosonde intercomparison (Nash et al., 2011) and are dominated by the sonde
812 type.

813 Statistics for Vaisala and Meteomodem radiosondes (manned and ARL) were produced. For Vaisala
814 we examined the German radiosondes (Figure 20) which form a relatively dense, well maintained
815 network with manned and ARL stations interspersed - ideal for this type of comparison. The
816 background uncertainties vary somewhat over time and regionally - they are probably slightly larger
817 over the UK because of the proximity of the North Atlantic. The Meteomodem samples were quite
818 small (from five French stations in total) and inconclusive; therefore, they will not be shown. No
819 attempts to provide a comparison of O-B statistics for Meisei ARL station were carried out. This is
820 due to the fact that all four Meisei ARLs are on small islands, three to the south of the main islands
821 of Japan and one to the south-east, whereas the manned stations are on the main islands (or two
822 distant islands). Therefore, the O-B comparison could be affected by differences in the
823 background uncertainties over the southern islands relative to the main islands.

824 Figure 21 shows the numbers of reports at standard levels for German RS92 launches in the period
825 2015-2017. There are more than twice as many manned launches as ARL ascents because four of
826 the manned stations usually report four times per day whereas the other four manned stations and
827 the five ARL stations report twice a day. One interesting feature is that the proportion of ARL ascents
828 reaching 20 hPa is significantly higher than the proportion of manned ascents. A plausible
829 explanation for this is that ARLs put less stress on the neck of the balloon than manual launches
830 (Tim Oakley, pers. comm. 2018). During the middle months of 2017, there was a transition from
831 Vaisala RS92 to Vaisala RS41 at German stations - the proportions of RS41 reports at different
832 standard levels (not shown) are very similar to those in Figure 20.

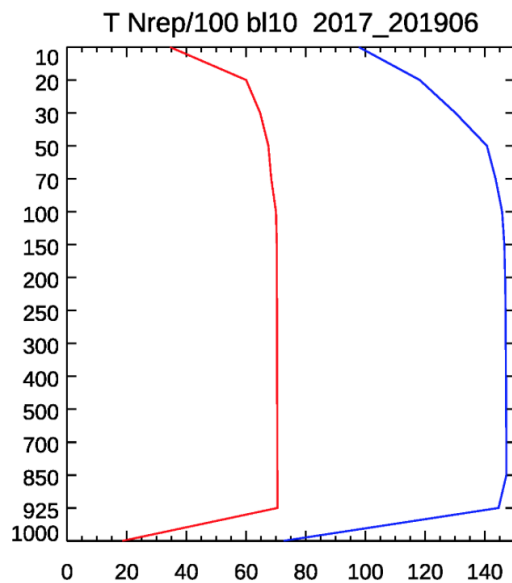
833



834

835 Figure 20: The main German radiosonde sites (two training/test sites not shown) and station identifiers: blue - manned
836 stations (8), red - autosondes (5), as in early 2019 and for several years before that.

837



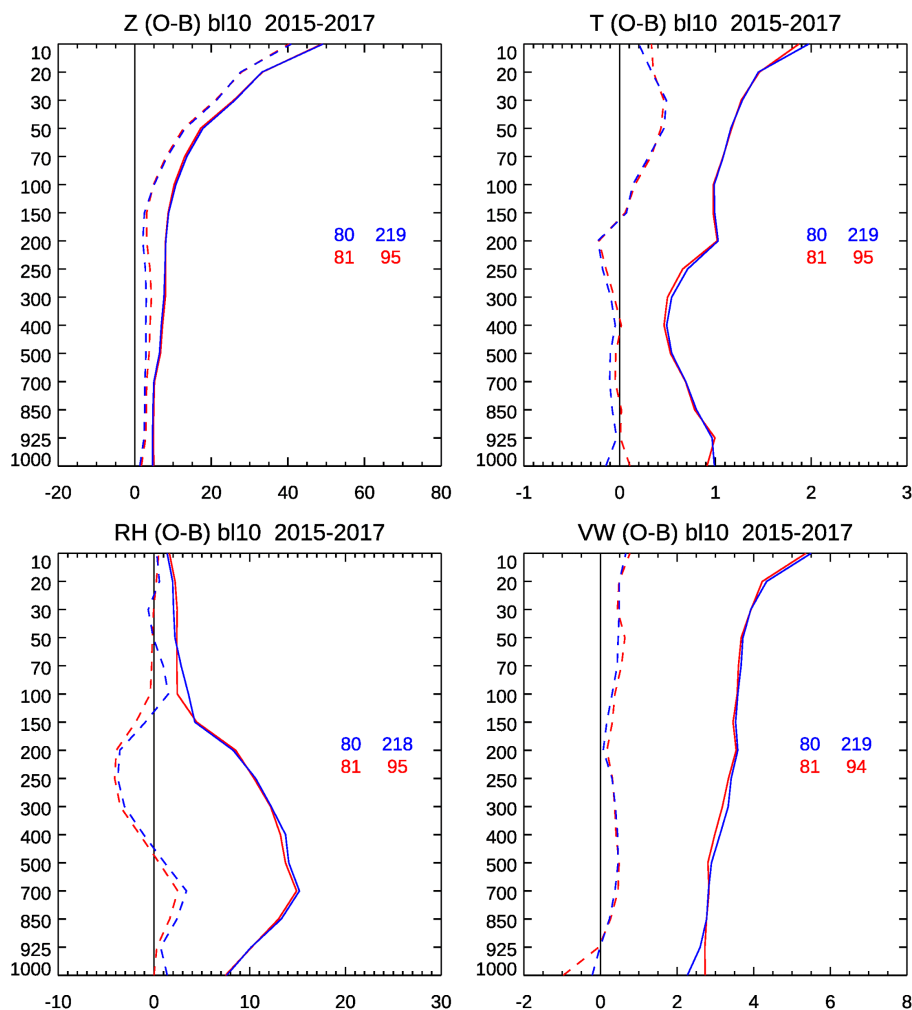
838

839 Figure 21. The number of temperature reports (hundreds) at standard levels, hPa, from German stations using Vaisala
840 RS92 radiosondes, 2015-2017: blue - manned stations, red - autosondes. The numbers for other variables are very
841 similar. There are fewer reports at 1000 hPa, and to some extent at 925 hPa, because these levels can be below the
842 launch site. The decrease at upper levels is due to balloon burst.

843



844 Figures 22 and 23 compare O-B mean and root-mean-square (rms) statistics for German RS92 and
845 RS41 reports respectively (for technical reasons alphanumeric TEMP reports were used rather than
846 binary BUFR reports, see Ingleby and Edwards, 2014). The RS92 results (Figure 22) are very similar
847 between manned and ARL stations (small differences at 1000 hPa are presumably due to the
848 proximity of the surface and relatively small samples). The upper tropospheric humidity has minor
849 systematic differences probably due to humidity time-lag and radiation corrections being
850 introduced at different dates at different stations.
851

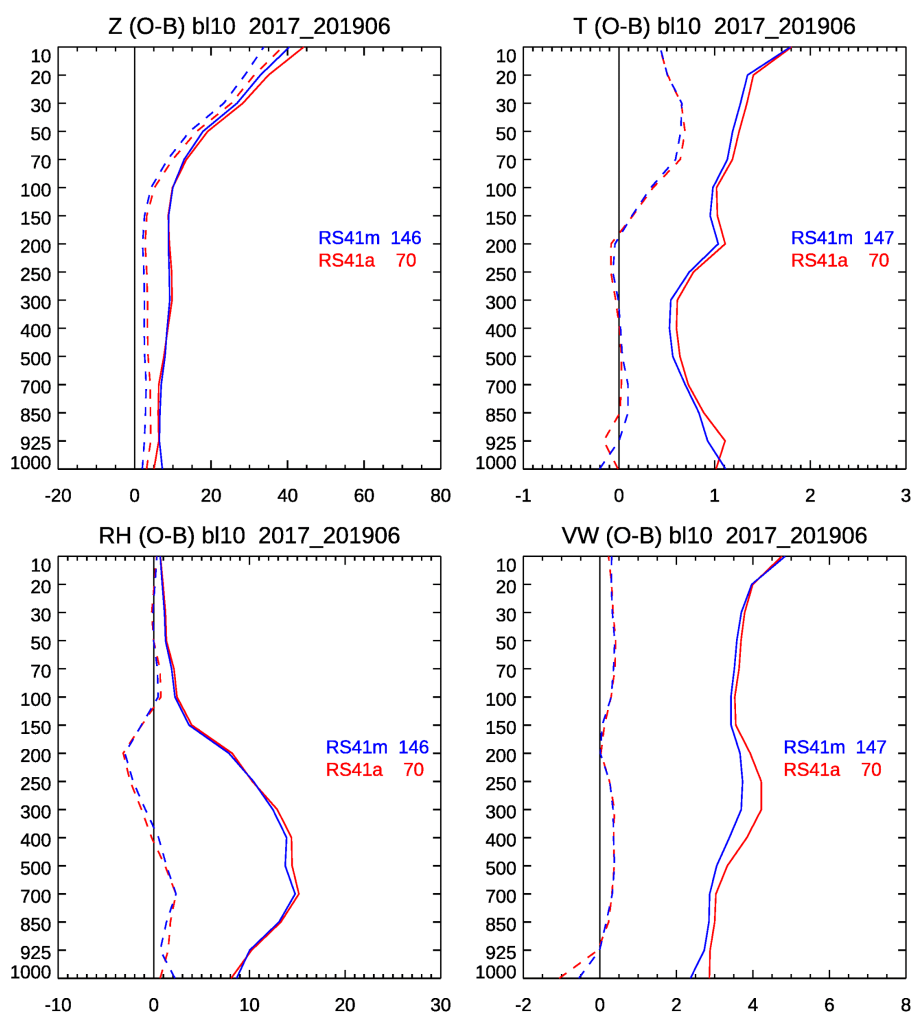


852
853 Figure 22: Mean (dashed) and rms (solid) O-B statistics for German RS92 ascents, 2015-2017: blue - manned, red - ARL.
854 Results for geopotential height (top left), temperature (top right), relative humidity (bottom left) and wind (mean wind
855 speed and rms vector wind; bottom right). The key gives the radiosonde code (80 for manual or 81 for ARL) and the
856 number of reports in hundreds.



857 In contrast and surprisingly, the RS41 results (Figure 23) show rather larger rms(O-B) differences for
858 ARL stations - especially for temperature and wind. Qualitatively similar results for RS41 are found
859 for subsets of the period considered confirming the robustness of the results. The reasons for the
860 larger ARL rms differences in Figure 23 are not clear yet; one possibility is linked to the accuracy of
861 the reported pressure values. Pressure is measured by the RS92. For the RS41-SG the pressure is
862 calculated starting from a surface pressure measurement, but the German stations use the RS41-
863 SGP with a pressure sensor. Discussions with Vaisala and DWD (the German weather service) have
864 not so far revealed the cause.

865



866

867 Figure 23: As Figure 22 but for RS41 reports, 2017-June 2019. For some months, all stations reported as type 23 (123
868 in BUFR) so they had to be separated using the station identifiers.

869



870 **7. Summary and discussion**

871 In this paper, the existing Automatic Radiosonde Launchers available on the market (Vaisala,
872 Meteomodem and Meisei) are presented and a first comparative analysis of the performance,
873 relative to the more prevalent practice of manual launches, for the two most mature systems at
874 present (Vaisala and Meteomodem) has been reported. The analysis is limited to the data available
875 from a few GRUAN certified or candidate sites (Sondakyla, Payerne, Trappes, Potenza, Faa'a) and to
876 the investigation of the O-B bias and rms using the ECMWF forecast model and the Vaisala ARLs and
877 manual stations of the DWD. The data analysis allows to infer the following principal conclusions:

- 878 ● From a technical point of view, the performance of ARL is fully similar or superior to that
879 achieved with the traditional manual launches due to the capability of the automatic
880 launchers to fully control several parameters during the different phases of the radiosonde
881 preparation and balloon launch. This reduces launch-to-launch variability typical in manual
882 launches.
- 883 ● Despite having some potential advantages, there are still some issues generating failure in
884 the launches which can be improved according to the feedback provided by the GRUAN
885 sites, operating mainly Vaisala ARLs, such as the not infrequent failure of the power supply
886 system or of the air conditioning system, plenty of issues related to the balloon release in
887 the vessel area, likely contributing to early balloon bursts, and to the management of the
888 gas flow to fill the balloon, while the ready-to-launch sondes storage area appears to be the
889 most efficient part of ARLs.
- 890 ● For both temperature and relative humidity, the GC correction has been investigated for
891 the Vaisala ARL, finding a negative offset relative to manual launch procedures at different
892 stations and considering different radiosonde types (RS92/RS41) and batches of a few
893 tenths of degree and % RH, respectively. For the Meteomodem ARL at Trappes station, the
894 difference between M10 temperature and humidity sensor and the Vaisala HMP110 housed
895 in the ARL, used as a reference immediately prior to launch shows a few tenths of degree
896 and % RH, respectively. These results need further investigation to understand the
897 underlying reasons and whether manual or ARL operations are closer to the observed
898 atmospheric profiles.
- 899 ● Systematic differences in the temperature profile for both Meteomodem and Vaisala are
900 smaller than ± 0.2 K up to 10 hPa; RH difference profile differences are smaller than 1% RH
901 for the Sodankylä Vaisala dataset up to 300 hPa, while it is constantly positive and smaller



902 than 2% for Faa'a station Meteomodem series. However, the restricted dataset available at
903 Faa'a station means caution should be applied in generalizing these results as representative
904 of all Meteomodem ARL.

905 ● O-B mean and rms statistics for German RS92 and RS41 are very similar between manned
906 and ARL stations. The upper tropospheric humidity has minor systematic differences
907 probably due to humidity time-lag and radiation corrections being introduced at different
908 dates at different stations. The RS41 sondes shows larger rms(O-B) differences for ARL
909 stations than RS92, in particular for temperature and wind. The accuracy of the reported
910 pressure values might be a possible reason to explain this difference.

911

912 As mentioned at the beginning of section 3, the factor limiting adoption of ARL radiosounding
913 products within the GRUAN reference network is mainly related to the use of an independent and
914 traceable calibration standards like the Standard Humidity Chamber (SHC) within the ARLs. At
915 present, for the different ARLs, this is possible but only before the sonde loading in the ARL trays.
916 GRUAN Data Processing (GDP) is currently applied to the ARL soundings performed by the GRUAN
917 stations though the related measurement programs cannot as yet be certified as GRUAN products.
918 The present analysis has provided a substantive move forwards towards this aim by showing that
919 performance is broadly comparable to manual launches.

920 In the last five years, several discussions within and outside the GRUAN community, involving also
921 the manufactures, allowed to identify a few possibilities to meet the full traceability for the ARLs.
922 Identified solutions to test are related to two main options:

923 ● Use of a SHC (plus a reference thermometer, such as PT100 sonde) immediately after the
924 manufacturer GC and prior to loading the sondes;

925 ● Use of reference thermometer and hygrometer within the the ready-to-launch sondes
926 storage area, as close as possible to the radiosonde sensors, with the optional use of a few
927 additional thermometers and hygrometers within the storage area to monitor the
928 uniformity of the temperature and relative humidity within the same area.

929 Both approaches have advantages and drawbacks. The first allows use of the SHC as a traceable
930 calibration standard at or around 100 % relative humidity, depending on the solution used in the
931 SHC. Nevertheless, the proposed two stage procedure can be applied only in advance of the launch
932 and tests are needed to confirm what was already shown in Section 4 at Sodankylä and Payerne



933 stations, i.e. a sonde can be launched within a few days from its upload in the ARL without differing
934 significantly from the SHC collected data.

935 The second approach can instead continuously monitor the radiosonde during the entire launch
936 procedure in the storage area and before the sonde tray is moved out to the vessel area for launch,
937 when temperature and RH within the storage area may rapidly change because of the incoming air
938 from outside the vessel area. This approach cannot directly use traceable calibration standards but
939 it must be based on the comparison with reference thermometers and hygrometers calibrated on
940 a routine and certified basis. In addition, the sonde calibration cannot be monitored at 100 % RH
941 because the air conditioning system within the ARL keeps stable humidity conditions and cannot be
942 modified to avoid an impact on the ARL operation efficiency.

943 For both the approaches above, a customized solution to collect the data and use them in the
944 generation of a GDP must be found given the constraints of the ARL software which does not allow
945 extra calibration or comparison values to be collected or saved in the main radiosonde launch files.
946 It must be noted that at 4 JMA stations, not belonging to GRUAN, the Vaisala ARL is used adopting
947 a modified setup of the AS15 system including an additional GC based on reference instruments
948 developed by Vaisala for temperature and humidity, i.e Vaisala HMP155 with HMT333, lodged in a
949 custom-made chamber. When loading the radiosonde, the JMA specified GC for temperature and
950 humidity is also performed, in line with JMA's rule for upper air observations, specifying that the
951 PTU radiosonde sensors should be compared to reference sensors before launch only to confirm
952 that the difference is within a pre-defined threshold, while reference values are not used for any
953 correction of the measured profiles. The JMA additional GC is not a traceable calibration standard
954 and does not allow to perform the 0% RH and 100% RH ground calibration immediately before the
955 launch. Instead, it can be made when the radiosonde is uploaded in the ARL using a method to save
956 the measured comparison values.

957 More details on the JMA specified ground check for temperature and humidity are available at:
958 <https://www.vaisala.com/sites/default/files/documents/RI41-Datasheet-B211322EN.pdf>.

959 The compilation of the table of ARL systems in Appendix A (also the plot in Figure 1) brought home
960 that it is not easy for users to know which stations are using ARLs. We recommend that information
961 on automated launchers (type, start date, end date if appropriate) should be included in the
962 OSCAR/Surface catalogue.

963 Other issues which must be considered and solved to provide a GDP from ARLs are related to the
964 need to supply the manufacturer software with an accurate local pressure measurement and its



965 height at the launch time. Delays between the actual and the reported launch time from the
966 software is another issue which is under investigation by GRUAN community.
967 The GRUAN community is discussing a strategy to achieve the full traceability for the ARL products
968 and to ascertain if any of the approaches described above can be tested intensively at one or more
969 sites: unfortunately, many of the GRUAN sites are also operational stations from the Met Services
970 and from other research institutions and are not readily available for testing. The next step will be
971 to identify which sites can perform specific tests on the ARL traceability and to collect as many
972 metadata as possible from all the GRUAN sites to report, in following publications, extensive
973 statistics validating the results presented in this paper.

974

975 **8. Acknowledgements**

976 Much useful information has been provided by the three manufacturers: Vaisala, Meteomodem and
977 Meisei. Information on which stations use Meteomodem ARLs was provided by Adrien Ferreira of
978 Meteomodem in April 2019. Hannu Jauhiainen of Vaisala provided a list of stations using their
979 Autosonde including several which were not known from the WIS reports. MeteoFrance and several
980 other National Meteorological Services have also provided information. The Faa'a data discussed in
981 this manuscript are available at ftp://ftp.lmd.polytechnique.fr/jcdupont/data_m10_gruan_faa and
982 can be used or cited under the DOI number <https://doi.org/10.14768/20181213001.1>.

983

984 **9. References**

- 985 Bodeker, G. E., Bojinski, S., Cimini, D., Dirksen, R., Haefelin, M., Hannigan, J. W., Hurst, D. F., Leblanc,
986 T., Madonna, F., Maturilli, M., Mikalsen, A., Philipona, R., Reale, T., Seidel, D., Tan, D., Thorne, P.,
987 Vömel, H. and Wang, J.: Reference upper-air observations for climate: From concept to reality,
988 *Bulletin of the American Meteorological Society*, 97 (1), pp. 123-135. doi: 10.1175/BAMS-D-14-
989 00072.1, 2016.
- 990
- 991 Carminati, F., Migliorini, S., Ingleby, B., Bell, W., Lawrence, H., Newman, S., Hocking, J., and Smith,
992 A.: Using reference radiosondes to characterise NWP model uncertainty for improved satellite
993 calibration and validation, *Atmos. Meas. Tech.*, 12, 83–106, [https://doi.org/10.5194/amt-12-83-](https://doi.org/10.5194/amt-12-83-2019)
994 2019, 2019.
- 995
- 996 Dirksen, R. J., Sommer, M., Immler, F. J., Hurst, D. F., Kivi, R., and Vömel, H.: Reference quality upper-
997 air measurements: GRUAN data processing for the Vaisala RS92 radiosonde, *Atmos. Meas. Tech.*, 7,
998 4463-4490, <https://doi.org/10.5194/amt-7-4463-2014>, 2014.
- 999
- 1000 Glisson, T. H.: *Introduction to Circuit Analysis and Design*, Springer Science & Business Media, Ed. 1,
1001 XV, 768, 10.1007/978-90-481-9443-8, 2011.
- 1002



- 1003 Haimberger, L., C. Tavalato, S. Sperka: Homogenization of the Global Radiosonde Temperature
1004 Dataset through Combined Comparison with Reanalysis Background Series and Neighboring
1005 Stations, *J. Clim.*, 25, 8108–8131, doi:10.1175/JCLI-D-11-00668.1, 2012.
- 1006
1007 Ho, S.-P., Peng, L., and Vömel, H.: Characterization of the long-term radiosonde temperature biases
1008 in the upper troposphere and lower stratosphere using COSMIC and Metop-A/GRAS data from 2006
1009 to 2014, *Atmos. Chem. Phys.*, 17, 4493–4511, <https://doi.org/10.5194/acp-17-4493-2017>, 2017.
- 1010
1011 Ingleby B, Edwards D.: Changes to radiosonde reports and their processing for numerical weather
1012 prediction, *Atmosph. Sci. Lett.*, 16: 44–49. doi: 10.1002/asl2.518, 2014
- 1013
1014 Ingleby, B.: An assessment of different radiosonde types 2015/2016. ECMWF Tech. Memo. 807, 69
1015 pp., [https://www.ecmwf.int/sites/default/files/elibrary/2017/17551-assessment-different-](https://www.ecmwf.int/sites/default/files/elibrary/2017/17551-assessment-different-radiosonde-types-20152016.pdf)
1016 [radiosonde-types-20152016.pdf](https://www.ecmwf.int/sites/default/files/elibrary/2017/17551-assessment-different-radiosonde-types-20152016.pdf), 2017.
- 1017
1018 Kobayashi, E., Hoshino, S., Iwabuchi, M., Sugidachi, T., Shimizu, K., and Fujiwara, M.: Comparison of
1019 the GRUAN data products for Meisei RS-11G and Vaisala RS92-SGP radiosondes at Tateno (36.06° N,
1020 140.13° E), Japan, *Atmos. Meas. Tech.*, 12, 3039–3065, <https://doi.org/10.5194/amt-12-3039-2019>,
1021 2019.
- 1022
1023 Kostamo, P., Advanced automation for upper-air stations, WMO Instruments and Observing
1024 Methods Report No. 49 (TECO-92), pp. 104–107.
1025 https://library.wmo.int/index.php?lvl=notice_display&id=11254#.Xeo3GS2h01l, 1992
- 1026
1027 Lehtinen, R., T. Tikkanen, J. Räsänen, and M. Turunen: Factors contributing to RS41 GPS-based
1028 pressure and comparison with RS92 sensor-based pressure, WMO Technical Conference (TECO), St.
1029 Petersburg, Russia. [https://www.wmo.int/pages/prog/www/IMOP/publications/IOM-116_TECO-](https://www.wmo.int/pages/prog/www/IMOP/publications/IOM-116_TECO-2014/Session%201/P1_28_Lehtinen_RS41PressCompRS92.pdf)
1030 [2014/Session%201/P1_28_Lehtinen_RS41PressCompRS92.pdf](https://www.wmo.int/pages/prog/www/IMOP/publications/IOM-116_TECO-2014/Session%201/P1_28_Lehtinen_RS41PressCompRS92.pdf), 2014.
- 1031
1032 Lilja A., Franssila J., Hautaniemi P., Lehmskero M. Review of the History and Future of Automatic
1033 Upper Air Soundings. TECO-2018, Amsterdam, the Netherlands. October 8th - 11th, 2018.
- 1034
1035 Madonna, F., Amodeo, A., Boselli, A., Cornacchia, C., Cuomo, V., D'Amico, G., Giunta, A., Mona, L.,
1036 and Pappalardo, G.: CIAO: the CNR-IMAA advanced observatory for atmospheric research, *Atmos.*
1037 *Meas. Tech.*, 4, 1191–1208, <https://doi.org/10.5194/amt-4-1191-2011>, 2011.
- 1038
1039 Madonna, F., Rosoldi, M., Güldner, J., Haefele, A., Kivi, R., Cadeddu, M. P., Sisterson, D., and
1040 Pappalardo, G.: Quantifying the value of redundant measurements at GCOS Reference Upper-Air
1041 Network sites, *Atmos. Meas. Tech.*, 7, 3813–3823, <https://doi.org/10.5194/amt-7-3813-2014>, 2014.
- 1042
1043 Nash J., T. Oakley, H. Vömel, and Wei Li.: WMO Intercomparison of High Quality Radiosonde
1044 Systems Yangjiang, China, 12 July - 3 August 2010, WMO Instruments and Observing Methods
1045 Report No. 107, 2011.
- 1046
1047 Sheppard, W. W., and C. C. Soule: Practical navigation, World Technical Institute, Jersey City, 1922.
- 1048



- 1049 Sherwood, S. C., C. L. Meyer, R. J. Allen, and H. A. Titchner: Robust tropospheric warming revealed
1050 by iterative homogenized radiosonde data, *J. Clim.*, 21, 5336–5352, doi:10.1175/2008JCL2320.1,
1051 2008.
- 1052
- 1053 Sofieva, V. F., F. Dalaudier, R. Kivi, and E. Kyrö: On the variability of temperature profiles in the
1054 stratosphere: Implications for validation, *Geophys. Res. Lett.*, 35, L23808,
1055 doi:10.1029/2008GL035539, 2008.
- 1056
- 1057 Thorne, P. W., D. E. Parker, S. F. B. Tett, P. D. Jones, M. McCarthy, H. Coleman, and P. Brohan:
1058 Revisiting radiosonde upper-air temperatures from 1958 to 2002. *J. Geophys. Res.*, 110, D18105,
1059 doi:10.1029/2004JD005753, 2005.
- 1060
- 1061

10. APPENDIX A: Table of ARL systems operating around the world

1063 Table A1: ARL stations shown in Figure 1. For each station, the WMO ID, which is also part of the WIGOS code
1064 (<https://oscar.wmo.int/surface>), the latitude, the longitude, the country and the period of installation is reported. For
1065 the approximate installation date (year or year-month), the metadata have been collected from different sources (IGRA,
1066 ECMWF, manufacturers, personal communication from scientists and instrument operators). If the last column is empty,
1067 no clear information on the installation period at that station are available. For Vaisala systems the "radiosonde type"
1068 in the reports should indicate if an ARL is being used, but it has been found that this is not always coded correctly. For
1069 Modem and Meisei systems there is no way for the current code formats to indicate that an ARL has been used. The
1070 list is ordered according to the WMO ID.

1071
1072

WMO ID	Latitude	Longitude	Country	Installed
01001	70.940	-8.668	Norway	Meteomodem 2019-09
01010	69.315	16.131	Norway	Vaisala 2014
01241	63.705	9.612	Norway	Vaisala 2001
01415	58.874	5.665	Norway	Vaisala 2013
01492	59.943	10.719	Norway	Vaisala 1997
02185	65.543	22.115	Sweden	Vaisala 1996
02365	62.532	17.436	Sweden	Vaisala 1994



02527	57.657	12.291	Sweden	Vaisala 1994
02591	57.671	18.345	Sweden	Vaisala pre-1996
02836	67.366	26.631	Finland	Vaisala 2005-12
02963	60.815	23.499	Finland	Vaisala 1998
03238	55.019	-1.878	UK	Vaisala 1999
03354	53.006	-1.250	UK	Vaisala 1999
03882	50.891	0.317	UK	Vaisala 2001
03918	54.503	-6.343	UK	Vaisala 2002
03953	51.939	-10.241	Ireland	Meteomodem 2015
04018	63.975	-22.588	Iceland	Vaisala 2006
04360	65.611	-37.637	Greenland	Meteomodem 2012
06610	46.813	6.943	Switzerland	Vaisala 2018
07110	48.444	-4.412	France	Meteomodem 2016-04
07145	48.770	2.020	France	Meteomodem 2015-04
07510	44.831	-0.691	France	Meteomodem 2012-06
07645	43.856	4.407	France	Meteomodem 2011-11
07761	41.918	8.792	France	Meteomodem 2014-06
08190	41.384	2.118	Spain	Meteomodem 2012



08221	40.465	-3.589	Spain	Vaisala 2002
08392	39.606	2.707	Spain	Vaisala 2002
08383	37.278	-6.911	Spain	Vaisala 2018
08430	38.002	-1.171	Spain	Meteomodem 2015
10035	54.527	9.550	Germany	Vaisala 2019-10
10113	53.712	7.152	Germany	Vaisala 2011
10410	51.404	6.968	Germany	Vaisala 2012
10548	50.562	10.377	Germany	Vaisala 2011
10739	48.828	9.201	Germany	Vaisala 2012
10868	48.245	11.553	Germany	Vaisala 2013
11010	48.232	14.201	Austria	Vaisala 2016
11120	47.260	11.355	Austria	Vaisala 2015
11240	46.994	15.447	Austria	Vaisala 2015
13388	43.327	21.898	Serbia	Meteomodem 2015
14430	44.101	15.339	Croatia	Vaisala 1999
16113	44.539	7.613	Italy	Vaisala 1999
16144	44.654	11.623	Italy	Vaisala 1998
45004	22.312	114.173	Hong Kong	Vaisala 2003



47155	35.170	128.573	S Korea	Vaisala 2001
47418	42.953	144.438	Japan	Vaisala 2010-03
47600	37.391	136.895	Japan	Vaisala 2010-03
47678	33.122	139.779	Japan	Meisei 2010-03 (Vaisala until 2003-06)
47741	35.458	133.066	Japan	Vaisala 2010-03
47778	33.45	135.757	Japan	Vaisala 2010-03
47909	28.393	129.552	Japan	Meisei 2007-03
47918	24.337	124.165	Japan	Meisei 2006-03
47945	25.829	131.229	Japan	Meisei 2017-03 (Vaisala until 2005-03)
60018	28.318	-16.382	Spain	Vaisala 2001
60096	23.705	-15.930	Morocco	Meteomodem 2012
60155	33.559	-7.667	Morocco	Meteomodem 2014
61980	-20.9	55.500	La Reunion	Meteomodem 2018-04
70026	71.287	-156.763	USA, Alaska	Vaisala 2010
70133	66.885	-162.597	USA, Alaska	Vaisala 2019
70200	64.513	-165.443	USA, Alaska	Vaisala 2019



70219	60.780	-161.838	USA, Alaska	Vaisala 2018
70231	62.953	-155.603	USA, Alaska	Vaisala 2018
70261	64.814	-147.859	USA, Alaska	Vaisala 2018
70273	61.175	-149.993	USA, Alaska	Vaisala 2018
70308	57.167	-170.22	USA, Alaska	Vaisala 2018
70326	58.678	-156.647	USA, Alaska	Vaisala 2019
70350	57.750	-152.494	USA, Alaska	Vaisala 2015
70361	59.503	-139.66	USA, Alaska	Vaisala 2018
70398	55.043	-131.571	USA, Alaska	Vaisala 2018
71964	60.733	-135.097	Canada	Vaisala 1997
78897	16.260	-61.510	Gadeloupe	Meteomodem 2015
81405	4.830	-52.370	French Guyana	Meteomodem 2012-09
89859	-74.624	164.232	Antarctic (S. Korea)	Vaisala 2014
91592	-22.27	166.450	New Caledonia	Meteomodem 2016-06



91938	-17.55	-149.6	Tahiti	Meteomodem 2018-10
94170	-12.678	141.921	Australia	Vaisala 1998
94302	-22.241	114.097	Australia	Vaisala 1997
94312	-20.373	118.632	Australia	Vaisala 1998
94332	-20.679	139.488	Australia	Vaisala 1998
94430	-26.613	118.536	Australia	Vaisala 1998
94510	-26.414	146.257	Australia	Vaisala 1998
94637	-30.784	121.454	Australia	Vaisala 2000
94653	-32.13	133.698	Australia	Vaisala 1999
94659	-31.156	136.805	Australia	Vaisala 2000
94711	-31.484	145.897	Australia	Vaisala 1997
94776	-32.793	151.836	Australia	Vaisala 2002
94821	-37.748	140.775	Australia	Vaisala 2010
94995	-31.542	159.077	Australia	Vaisala 2010
95527	-29.49	149.847	Australia	Vaisala 1999
96996	-12.189	96.834	Australia	Vaisala 1997

1073
1074
1075
1076
1077
1078



1079 Table A2: Additional ARL systems not transmitting data through the WIS in 2019 or used only for tests and short
1080 campaign (not shown in Figure 1). The ARL from 08160 was relocated to 08383.
1081

Identifier	Latitude	Longitude	Country	Installed
POT (GRUAN)	40.600	15.725	Italy	Vaisala 2004
08160	41.660	-1.000	Spain	Vaisala 2005 to 2016
72402 (test)	37.930	-75.480	USA	Vaisala 2014 Meteomodem 2017
71461 (test)	55.810	-117.890	Canada	Vaisala 2016 Meteomodem 2017
10141 (test)	53.650	10.117	Germany	Vaisala 2016

1082